JOC Article
pubs.acs.org/joc

Ultrafast Light-Driven Nanomotors Based on an Acridane Stator

Artem A. Kulago,[†] Emile M. Mes,[‡] Martin Klok,[†] Auke Meetsma,[†] Albert M. Brouwer,[‡] and Ben L. Feringa*,[†]

[†]*Center for Systems Chemistry, Stratingh Institute for Chemistry, Faculty of Mathematics and Natural Sciences, University of Groningen, Nijenborgh 4, 9747 AG Groningen, The Netherlands and* [‡]*Van't Hoff Institute of Molecular Sciences, University of Amsterdam, Nieuwe Achtergracht 129, 1018 WS Amsterdam, The Netherlands*

b.l.feringa@rug.nl

Received October 14, 2009

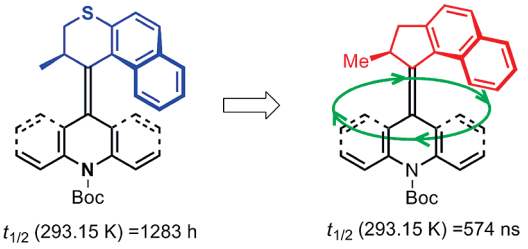

$t_{1/2}$ (293.15 K) =1283 h $t_{1/2}$ (293.15 K) =574 ns

A series of molecular motors featuring a symmetrical acridane stator is reported. Photochemical and thermal isomerization experiments confirm that this stator, in combination with a thiopyran rotor, results in molecular rotary motion in which the rate-determining thermal helix inversion proceeds effectively only at temperatures above 373 K. The introduction of a cyclopentanylidene rotor unit results in a decrease in steric hindrance with respect to the stator, and as a consequence, a 10^{12}-fold increase in the rate of thermal helix inversion is observed. Nanosecond transient absorption spectroscopy allows for the thermal processes to be followed accurately at ambient temperature. The rotary motor is shown to be able to operate at 0.5 MHz rotational frequencies under optimal conditions.

Introduction

Biomolecular motors are arguably among the most fascinating systems in nature and are involved in nearly every key biological process.[1] The rotary ATP synthase motor,[2] linear kinesin and myosin motors,[3] and RNA polymerase[4] convert chemical energy into mechanical work on a biomolecular level, and the bacterial flagellar rotary motor,[5] which induces propulsion of the whole bacterial cell, is among the most prominent example. Although operational mechanisms are different, these motions are reminiscent of the dynamics of macroscopic mechanical machines.[6] Biomotors display high efficiency[7] featuring complex protein structures, and it is challenging to reproduce their function in synthetic mechanical systems. In construction of artificial mechanical devices, such as motors at the molecular level,[8] one is confronted with

(1) Schliwa, M. *Molecular Motors*; Wiley-VCH: Weinheim, Germany, 2002.
(2) (a) Boyer, P. D. *Angew. Chem., Int. Ed.* **1998**, *37*, 2296–2307. (b) Walker, J. E. *Angew. Chem., Int. Ed.* **1998**, *37*, 2308–2319. (c) Boyer, P. D. *Nature* **1999**, *402*, 247–249.
(3) (a) Finer, J. T.; Simmons, R. M.; Spudich, J. A. *Nature* **1994**, *368*, 113–119. (b) Kitamura, K.; Tokunaga, M.; Iwane, A. H.; Yanagida, T. *Nature* **1999**, *397*, 129–134. (c) Wells, A. L.; Lin, A. W.; Chen, L.-Q.; Safer, D.; Cain, S. M.; Hasson, T.; Carragher, B. O.; Milligan, R. A. H.; Sweeney, L. *Nature* **1999**, *401*, 505–508. (d) Molloy, J. E.; Schmitz, S. *Nature* **2005**, *435*, 285–287. (e) Carter, N. J.; Cross, R. A. *Nature* **2005**, *435*, 308–312.
(4) (a) Abbondanzieri, E. A.; Greenleaf, W. J.; Shaevitz, J. W.; Landick, R.; Block, S. M. *Nature* **2005**, *438*, 460–465. (b) Li, J. J.; Tan, W. *Nano Lett.* **2002**, *2*, 315–318. (c) Bath, J.; Green, S. J.; Turberfield, A. J. *Angew. Chem., Int. Ed.* **2005**, *44*, 4358–4361. (d) Yurke, B.; Turberfield, A. J.; Mills, A. P.; Simmel, F. C.; Neumann, J. L. *Nature* **2000**, *406*, 605–608. (e) Harada, Y.; Ohara, O.; Takatsuki, A.; Itoh, H.; Shimamoto, N.; Kinosita, K. *Nature* **2001**, *409*, 113–115.
(5) (a) Kinbara, K.; Aida, T. *Chem. Rev.* **2005**, *105*, 1377–1400. (b) Berg, H. C. *Annu. Rev. Biochem.* **2003**, *72*, 19–54. (c) Chen, X.; Berg, H. C. *Biophys. J.* **2000**, *78*, 1036–1041. (d) Xing, J.; Bai, F; Berry, R.; Oster, G. *Proc. Natl. Acad. Sci. U.S.A.* **2006**, *103*, 1260–1265.
(6) Goodsell, D. S. *Our Molecular Nature, The Body's Motors, Machines and Messages*; Springer-Verlag: New York, 1996.
(7) (a) van den Heuvel, M. G. L.; Dekker, C. *Science* **2007**, *317*, 333–336. (b) Yasuda, R.; Noji, H.; Kinosita, K.; Yoshida, M. *Cell* **1998**, *93*, 1117–1124. (c) Mehta, A. D.; Rock, R. S.; Rief, M.; Spudich, J. A.; Mooseker, M. S.; Cheney, R. E. *Nature* **1999**, *400*, 590–593. (d) Kinosita, K.; Yasuda, J. R.; Noji, H.; Adachi, K. *Philos. Trans. R. Soc. London, Ser. B* **2000**, *355*, 473–489. (e) Schmiedl, T.; Seifert, U. *Europhys. Lett.* **2008**, *83*, 30005-1–30005-5.
(8) (a) Eric, D. K. *Nanosystems: Molecular Machinery, Manufacturing, and Computation*; Wiley: New York, 1992. (b) Porto, M.; Urbakh, M.; Klafter, J. *Phys. Rev. Lett.* **2000**, *84*, 6058–6061. (c) Gimzewski, J. K.; Joachim, C. *Science* **1999**, *283*, 1683–1688.

Published on Web 12/23/2009 DOI: 10.1021/jo902207x

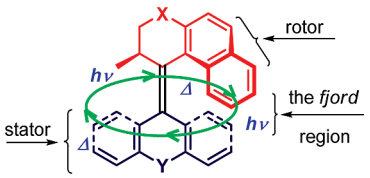

FIGURE 1. General structure of second-generation molecular motors.

some of the most demanding problems in modern science.[9] Nevertheless, various approaches to synthetic molecular machines have been reported, functioning by the virtue of rotation around a single or double bond, by conformational changes, or by change in noncovalent interactions, and attempts to modulate the translational and rotational motion of different parts of molecules have been reported.[10,11]

Overcrowded alkene-based rotary motors are synthetic molecular motors that display unidirectional, 360° rotation around a central double bond that functions as axle of rotation (Figure 1).[12] Their function is dependent on some key features displayed by these structures: an intrinsic helical shape, an alkene moiety that can undergo photoisomerization, and a stereogenic center with a methyl substituent in the rotor part that adopts an energetically preferred pseudoaxial orientation due to steric hindrance with the stator unit. The unidirectional rotation of the upper rotor with the respect to the lower stator is achieved by a combination of two energetically uphill photochemical *cis*−*trans* isomerizations each followed by an energetically downhill thermal step. Upon irradiation, *cis*−*trans* isomerization occurs with concomitant inversion of the helicity, changing the configuration of the rotor. This forces the methyl substituent in the rotor to adopt a less favored pseudoequatorial orientation, with increased energy relative to the pseudoaxial orientation. To revert to the most favored pseudoaxial conformation, the rotor must slip over the stator, again inverting helicity. This process results in an irreversible thermal isomerization, the direction of which is dictated by the absolute configuration at the stereogenic center. The energy barrier for this thermal isomerization is the rate-determining step of the rotation cycle and depends, among others, on the steric hindrance in the "*fjord* region" of the molecule (Figure 1). Other factors that influence the height of this barrier include the twist in the central double bond[13] and the electronic properties of the substituents in conjugation with the central double bond (the axle of rotation).[14] It is evident that there is a delicate balance between the nature of the substituents and the effect on the isomerization process governing the rotary behavior. A general strategy to introduce suitable functional groups that allow anchoring of rotary motors for incorporation into multicomponent mechanical systems is also highly warranted. The design, synthesis, and rotary behavior of new motors that will allow for ready functionalization and in which a large change in rotary speed is achieved is outlined in this paper.

Molecular Design

The successful demonstration of unidirectional rotary motion in a molecular motor as shown in Figure 1 raised the question whether these structures would be suitable for immobilization onto surfaces or incorporated as a part of multicomponent systems. Ultimately, this will be required if molecular machinery are to be constructed in which the dynamic properties are based on the functioning of the rotor. Also, the control of the rotary speed continues to be an important issue in the design of the motor.[15] For this reason, structural modification and functionalization of second-generation molecular motors has been investigated extensively in our group, and the development of assemblies of light-driven rotary motors chemically bound to nanoparticles and surfaces has been accomplished.[16] In this respect, one challenge we envision that has to be addressed in view of future applications of the second-generation molecular motors is to maintain the symmetry of the lower half. While keeping proper substituents for attachment, one has to avoid the formation of *cis*−*trans* isomers during preparation, as this complicates unequivocal assignment of the isomerization processes or requires tedious isomer separation. On the other hand, straightforward synthesis of molecular motors with stator parts equally functionalized on each side rests on a substantial number of synthetic steps, while only a limited number of convenient substituents for the direct attachment of functional groups are available.[17] For this reason, a redesign of second-generation molecular motors has focused on a system which displays a symmetrically functionalizable stator without the requirement of a large number of synthetic steps. The central Y atom seems an appropriate position to achieve this goal (Figure 1).

The N-Boc-protected acridane stator was chosen due to its symmetric structure and the ability to easily introduce different pending groups, suitable for construction of various motor systems after deprotection (Figure 2).

Key to the successful utilization of molecular motors is the possibility to control the rate of rotation.[18] Acceleration of the rotary motion can be achieved by lowering the energy of the thermal isomerization barriers as the speed of the full rotation cycle is theoretically limited by the rate-determining

(9) Browne, W. R.; Feringa, B. L. *Nat. Nanotechnol.* **2006**, *1*, 25–35.
(10) For the reviews on synthetic molecular motors, see: (a) Balzani, V.; Venturi, M.; Credi, A. *Molecular Devices and Machines: A Journey Into the Nanoworld*; Wiley-VCH: Weinheim, Germany, 2006. (b) Kay, E. R.; Leigh, D. A.; Zerbetto, F. *Angew. Chem., Int. Ed.* **2007**, *46*, 72–191.
(11) (a) Feringa, B. L. *J. Org. Chem.* **2007**, *72*, 6635–6652. (b) Kottas, G. S.; Clarke, L. I.; Horinek, D.; Michl, J. *Chem. Rev.* **2005**, *105*, 1281–1376. (c) Kelly, T. R; Cai, X.; Damkaci, F.; Panicker, S. B.; Tu, B.; Bushell, S. M.; Cornella, I.; Piggot, M. J.; Salives, R.; Cavero, M.; Jasmin, S. *J. Am. Chem. Soc.* **2007**, *129*, 376–386.
(12) (a) Koumura, N.; Geertsema, E. M.; van Gelder, M. B.; Meetsma, A.; Feringa, B. L. *J. Am. Chem. Soc.* **2002**, *124*, 5037–5051. (b) Pollard, M. M.; Klok, M.; Pijper, D.; Feringa, B. L. *Adv. Funct. Mater.* **2007**, *17*, 718–729.
(13) Vicario, J.; Walko, M.; Meetsma, A.; Feringa, B. L. *J. Am. Chem. Soc.* **2006**, *128*, 5127–5135.
(14) (a) Pijper, D.; van Delden, R. A.; Meetsma, A.; Feringa, B. L. *J. Am. Chem. Soc.* **2005**, *127*, 17612–17611. (b) Pollard, M. M.; Wesenhagen, P. V.; Pijper, D.; Feringa, B. L. *Org. Biomol. Chem.* **2008**, *6*, 1605–1612.
(15) Pollard, M. M.; Meetsma, A.; Feringa, B. L. *Org. Biomol. Chem.* **2008**, *6*, 507–512.
(16) (a) van Delden, R. A.; Wiel, M. K.; Pollard, M. M.; Vicario, J.; Koumura, N.; Feringa, B. L. *Nature* **2005**, *437*, 1337–1340. (b) Pollard, M. M.; Lubomska, M.; Rudolf, P.; Feringa, B. L. *Angew. Chem., Int. Ed.* **2007**, *46*, 1278–1280. (c) Katsonis, N.; Lubomska, M.; Pollard, M. M.; Feringa, B. L.; Rudolf, P. *Prog. Surf. Sci.* **2007**, *82*, 407–434.
(17) (a) ter Wiel, M. K.; Feringa, B. L. *Synthesis* **2005**, *11*, 1789–1797. (b) Pollard, M. M.; ter Wiel, M. K.; van Delden, R. A.; Vicario, J.; Koumura, N.; Brom, C. R.; Feringa, B. L. *Chem.—Eur. J.* **2008**, *14*, 11610–11622.
(18) Klok, M.; Walko, M.; Geertsema, E. M.; Ruangsupapichat, N.; Kistemaker, J. C. M.; Meetsma, A.; Feringa, B. L. *Chem.—Eur. J.* **2008**, *14*, 11183–11193.

SCHEME 1. Synthesis of Second-Generation Molecular Motors (1, *cis*-3, *trans*-3)[a]

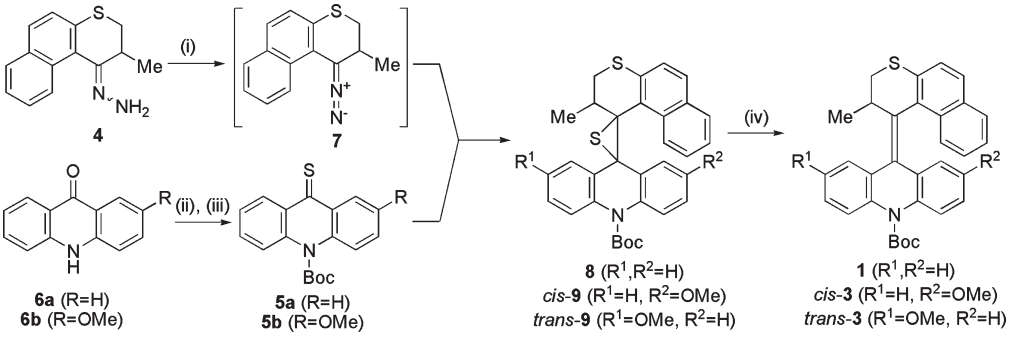

[a]Key: (i) MnO_2, $MgSO_4$, KOH (sat. aq.)/MeOH/CH_2Cl_2, 0 °C, 67−69%; (ii) DMAP, Boc_2O, CH_3CN, rt, 68−70%; (iii) Lawesson's reagent, THF, 60 °C, 80−83%; (iv) (4-MeO-C_6H_4)$_3$P, toluene, reflux, 85−89%.

steps of helix inversion.[19] Recent results indicate that decrease of steric hindrance in the fjord region by the substitution of a thiopyran six-membered ring-based rotor for a cyclopentanylidene five-membered ring-based rotor decreases this barrier considerably,[20] allowing rates for the thermal processes of up to 10^6 s^{-1} to be reached.

In this study, the synthesis of new molecular motors using acridane-based stators is described to provide a basis for future functionalization of motors via the central nitrogen atom. An extensive analysis of the rotaty behavior of these systems comprising an acridane-based stator coupled to thiopyran- and cyclopentanylidene rotors is reported using NMR, UV/vis, and CD spectroscopy in combination with nanosecond transient differential absorption spectroscopy.

Results and Discussion

Synthesis of Second-Generation Molecular Motors (1, *cis*-3, *trans*-3). The new type of molecular motors contains a chiral 2,3-dihydromethonaphtho[2,1-*b*]thiopyran rotor and a N-Boc-protected stator (Figure 2). The synthesis of the 2,3-dihydromethyl-1*H*-naphtho[2,1-*b*]thiopyran-1-one hydrazone **4** has been previously reported from cheap and readily available starting materials.[11a] *tert*-Butyl-9-thioxoacridine-10(9*H*)-carboxylate **5a** and 2-methoxy-substituted analogue **5b** as precursors of the stator (Scheme 1) were easily prepared in two steps by initial treatment of the corresponding acridin-9(10*H*)-one **6a** or its 2-methoxy derivative **6b** with di-*tert*-butyl dicarbonate in the presence of DMAP as a base. Subsequent conversion to the desired thioketones was performed by the use of Lawesson's reagent in THF at reflux.[21]

The diazo-thioketone coupling reaction[22] has been proven to be a successful method to connect the stator and rotor of second-generation molecular motors. In the diazo-thioketone approach, strain between the two parts is gradually introduced via a 1,3-dipolar cycloaddition under formation of an unstable five-membered thiadiazolidine moiety, followed by a nitrogen extrusion to yield the three-membered episulfide. In a separate step, a sulfur elimination process

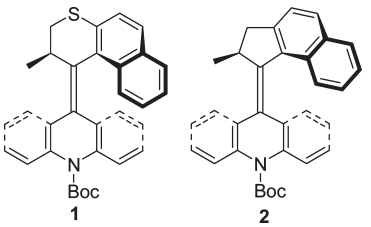

FIGURE 2. Molecular rotary motors **1** and **2**.

provides the overcrowded alkene. Hydrazone **4** was oxidized to the unstable, purple diazo compound **7** using manganese-(IV) dioxide in the presence of catalytic amounts of base in dichloromethane at 0 °C, and subsequent addition of thioketone **5a** gave episulfide **8** (Scheme 1). Desulfurization of the intermediate was performed by heating at reflux in toluene in the presence of tris(4-methoxyphenyl)phosphine, providing **1** carrying a symmetrical stator. The use of thioketone **5b** in the same sequence provided a mixture of *cis*-**9** and *trans*-**9** as a white solid (*cis*/*trans* ratio 1.7:1). This mixture was used in the desulfurization reaction to provide a mixture of *cis*-**3** and *trans*-**3**. The isomers were separated by flash column chromatography (silica gel, *n*-pentane/ether = 10:1) to yield pure *cis*-**3** (50%) and *trans*-**3** (37%). The new alkenes **1**, *cis*-**3**, and *trans*-**3** were fully characterized by ^{1}H and ^{13}C NMR spectroscopy and HRMS. The ^{1}H NMR spectra of both *cis*-**3** and *trans*-**3** display a shift of the methyl substituent at the stereogenic center to 0.51 ppm, due to aromatic ring anisotropy. The protons at the 2′-position are found at 3.99 ppm (*cis*-**3**) and 4.09 ppm (*trans*-**3**), respectively (see Scheme 2 for proton numbering in the stator). The assignment of the *trans* and *cis* geometry around the central double bond was possible based on distinct differences between their ^{1}H NMR spectra (Table 1). The singlets representing the methoxy substituents are found at 3.35 ppm (*trans*-**3**) and 2.73 ppm (*cis*-**3**). To determine the relative orientation of the methyl group at the stereogenic center, ^{1}H NMR spectra of both *trans*- and *cis*-isomers were studied in detail. Coupling constants of H(2′) and H(3′) of 2.4 and 6.8 Hz were found, indicating that the methyl groups at the 2′-position of both isomers adopt a pseudoaxial orientation.[23] Enantioresolution of racemic **1** was performed by preparative chiral HPLC (Chiralpak AD) under normal phase

(19) Geertsema, E. M.; der Molen, S. J.; Martens, M.; Feringa, B. L. *Proc. Natl. Acad. Sci. U.S.A.* **2009**, *106*, 16919–16924.
(20) Klok, M.; Boyle, N.; Pryce, M. T.; Meetsma, A.; Browne, W. R.; Feringa, B. L. *J. Am. Chem. Soc.* **2008**, *130*, 10484–10485.
(21) Ozturk, T.; Ertas, E.; Mert, O. *Chem. Rev.* **2007**, *107*, 5210–5278.
(22) (a) Barton, D. H. R.; Willis, B. *J. Chem. Soc., Perkin Trans. 1* **1972**, 305–310. (b) Buter, J.; Wassenaar, S.; Kellogg, R. M. *J. Org. Chem.* **1972**, *37*, 4045–4060.
(23) Karplus, M. *J. Am. Chem. Soc.* **1963**, *85*, 2870–2871.

SCHEME 2. Photochemical and Thermal Isomerization of 1

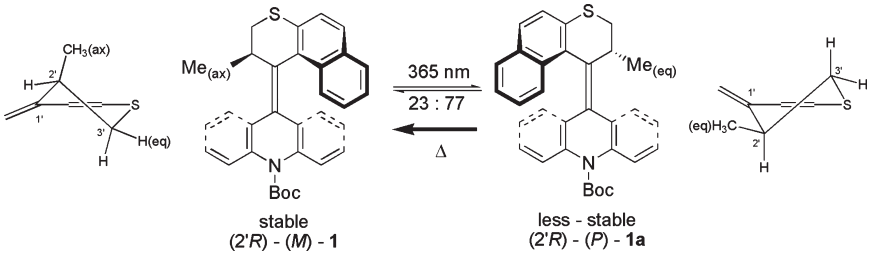

TABLE 1. Selected ^{1}H NMR Data of 1, 1a, *cis*-3, *cis*-3a, *trans*-3, and *trans*-3a in Toluene-d_8

	chemical shift, ppm			coupling constants
compound[a,b]	MeO	Me	H(2′)	$J_{H(2')-H(3')}$, Hz
1		0.50	3.98	2.44, 6.84
1a		0.97	2.27	6.84, 12.21
cis-**3**	2.73	0.51	3.99	2.44, 6.83
cis-**3a**	2.69	0.97	2.30	7.32, 12.21
trans-**3**	3.35	0.51	4.09	2.44, 6.83
trans-**3a**	3.28	1.08	2.29	7.32, 12.21

[a]Structures are represented in Schemes 1 and 2. [b]The *cis*-**3a** and *trans*-**3a** represent the less stable isomers (vide infra).

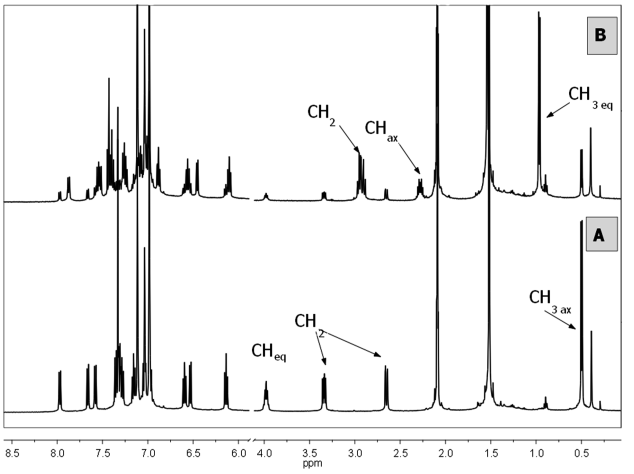

FIGURE 3. ^{1}H NMR spectra (toluene-d_8) of (A) **1** and (B) photostationary state mixture of **1** and **1a** after irradiation at 355 nm.

conditions using heptane/2-propanol = 99:1 as eluent at 50 °C. The absolute configuration of the second fraction was assigned as (2′*R*)-(*M*)-**1**, by comparison of the CD spectrum with those of related compounds.[24]

Photochemical and Thermal Switching of 1, *cis*-3, and *trans*-3. The photochemical and thermal isomerization of overcrowded alkenes **1**, *cis*-**3**, and *trans*-**3** was studied by ^{1}H NMR spectroscopy using racemic mixtures (Figure 3). Irradiation of a solution of **1** in toluene-d_8 ($c = 3.14 \times 10^{-3}$ M) was performed using UV light at 365 nm at 20 °C. A photostationary state (PSS) with a ratio of 23:77 of starting material (**1**)/product (**1a**) was reached after 4 h (Scheme 2).

The ^{1}H NMR spectra of the product **1a** resulting from irradiation of **1** displayed a shift of the absorption of the

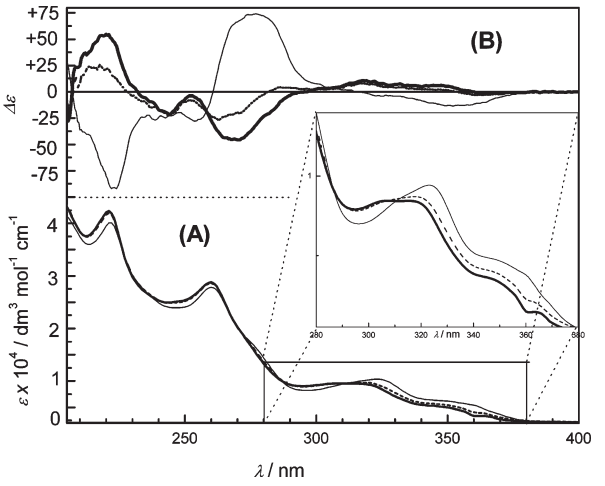

FIGURE 4. (A) UV/vis and (B) CD spectra (*n*-hexane) of stable (2′*R*)-(*M*)-**1** (solid line) and the photostationary state mixture of (2′*R*)-(*M*)-**1** and (2′*R*)-(*P*)-**1a** after irradiation at 312 nm (dotted line) and 355 nm (bold line).

methyl substituent at the 2′-position of the rotor to 0.97 ppm. The signal of the proton at the 2′-position shifted to 2.27 ppm (Table 1). Coupling constants of 12.21 and 6.84 Hz were found for H(2′) and H(3′) in **1a**, indicating that the methyl substituent at the 2′-position of this isomer adopts a pseudoequatorial orientation. Heating the photostationary mixture solution to 80 °C for 12 h resulted in quantitative conversion of **1a** into the stable isomer **1** as the ^{1}H NMR spectrum of the initial isomer was fully restored. Changing the irradiation wavelength to 312 nm resulted in establishing a different photostationary state with a less favorable ratio of 47:53 of starting material **1**/product **1a**, confirming the photoreversible nature of the process.[25]

In a similar manner, the photoisomerization of enantiomerically pure (2′*R*)-(*M*)-**1** was followed using UV/vis and circular dichroism (CD) spectroscopy (Figure 4). A sample of (2′*R*)-(*M*)-**1** in *n*-hexane was irradiated at 20 °C with 365 nm light, resulting in a decrease in the absorption in the 312−380 nm range of the UV/vis spectrum and an inversion of the sign of the main CD absorptions at 218, 270, and 346 nm.

The change in sign of the major CD absorptions reflects the inversion of the *M* to the *P* helix. As several isosbestic points were observed in both CD and UV/vis spectra, no degradation and/or side reactions occurred during the photochemical isomerization process. The kinetic and ther-

(24) (a) Koumura, N.; Geertsema, E. M.; Meetsma, A.; Feringa, B. L. *J. Am. Chem. Soc.* **2000**, *122*, 12005–12006. (b) Fujita, T.; Kuwahara, S.; Harada, N. *Eur. J. Org. Chem.* **2005**, *2005*, 4533–4543.

(25) Fujita, T.; Kuwahara, S.; Harada, N. *Eur. J. Org. Chem.* **2005**, *2005*, 4544–4556.

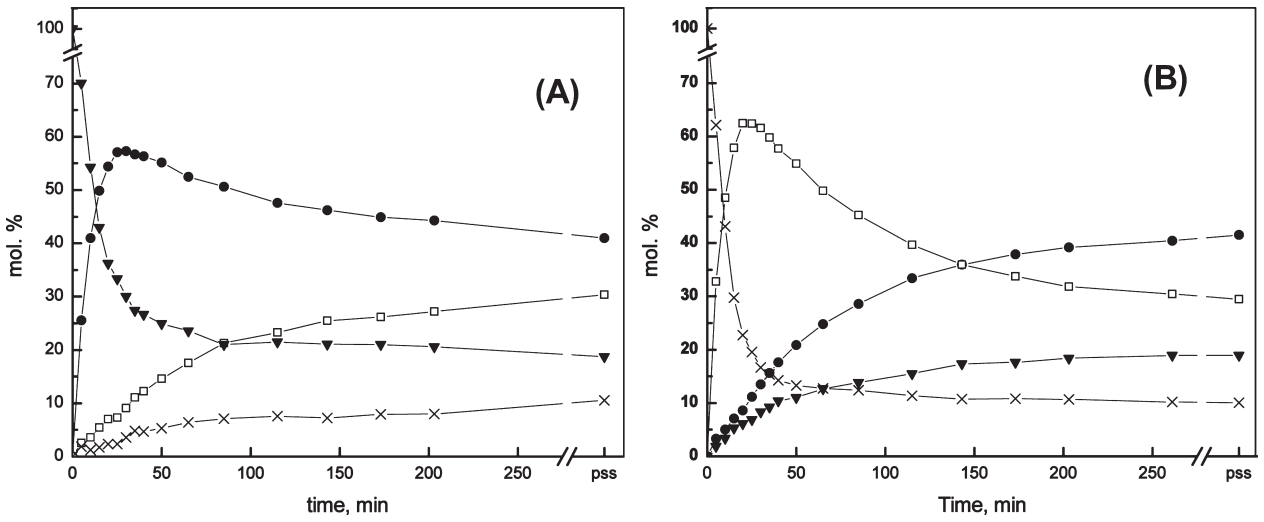

FIGURE 5. Changes of the molar ratios of the isomers (−×− *trans*-**3**; −□− *cis*-**3a**; −●− *trans*-**3a**; −▼− *cis*-**3**) with time upon irradiation of (A) *cis*-**3** and (B) *trans*-**3** in toluene solutions.

modynamic parameters[26] of the reverse thermal isomerization of less stable **1a** into stable **1** isomer were determined by ^{1}H NMR by monitoring the change in intensities for the methyl substituents at the 2′-position for both forms over the range of 333.15−383.15 K: $\Delta^{\ddagger}G^{\circ} = 110.1 \pm 0.1$ kJ·mol^{-1} ($\Delta^{\ddagger}H^{\circ} = 103.4 \pm 0.3$ kJ·mol^{-1}, $\Delta^{\ddagger}S^{\circ} = -23.3 \pm 0.9$ J·mol^{-1}·K^{-1}, $E_a = 106.3 \pm 0.1$ kJ·mol^{-1}, $A = (1.2 \pm 0.1) \times 10^{12}$ s^{-1}, $t_{1/2}$ (20 °C) = 1283 ± 163 h, k (20 °C) = $(1.5 \pm 0.2) \times 10^{-7}$ s^{-1}).

Motor molecule **1** contains a symmetric lower half, and as a result, just one photochemical and one thermal isomerization step, each accompanied by a helix inversion, converts the unstable alkene to its initial stable isomer, making together the photochemical−thermal equilibrium during motor functioning. To be able to get more insight into the rotation cycle, solutions of asymmetric (MeO substituents in stator) *cis*-**3** and *trans*-**3** isomers in toluene-d_8 were irradiated with 365 nm light at 0 °C separately, and the progress of the reactions was monitored by ^{1}H NMR spectroscopy in time.

Upon irradiation of *cis*-**3** for 0.5 h (Figure 5A), an initial rapid reduction in concentration of the starting material was observed with the concomitant appearance of a new isomer. The ^{1}H NMR spectrum of this newly formed less stable isomer revealed that the absorption of the methyl substituent at the 2′-position was shifted downfield to 1.08 ppm and the signal of the proton at the 2′-position was shifted to 2.29 ppm (Figure 6). Notably, the absorption of the methoxy group at the stator was shifted downfield to 3.28 ppm, which is close to the absorption of stable *trans*-**3** (3.35 ppm). Coupling constants of 12.21 and 7.32 Hz were found for the H(2′) and H(3′) protons, indicating that the methyl substituent adopts a pseudoequatorial orientation in the newly formed isomer, which was assigned to be the less stable *trans*-**3a** isomer (Table 1). However, upon prolonged irradiation, the concentration of the less stable *trans*-**3a** went through a maximum and then decreased, while at the same time, the formation of two new isomers was observed. By comparison of the ^{1}H NMR spectra, one of these was identified as the stable *trans*-**3** isomer. The other formed isomer displayed a shift

(26) See Supporting Information in ref 12a for experimental details.

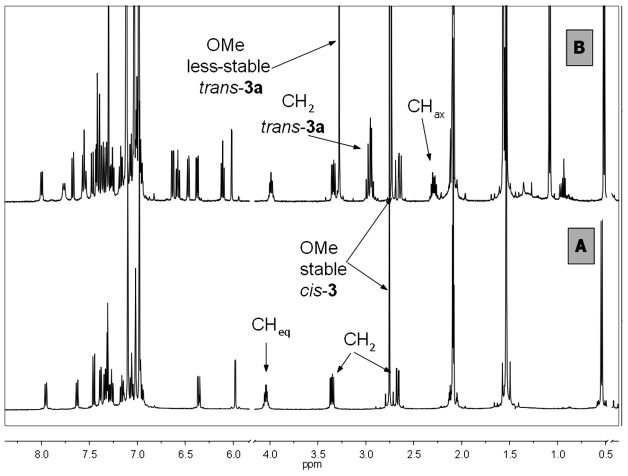

FIGURE 6. ^{1}H NMR spectra (toluene-d_8) of *cis*-**3** (A) before and (B) after irradiation at 355 nm (30 min).

of the methyl substituent at the 2′-position downfield to 0.97 ppm. The signals of the proton at the 2′-position were shifted upfield to 2.30 ppm, and the adsorption of the methoxy group at the rotor was shifted upfield to 2.69 ppm, close to the shift of the initial form, the stable *cis*-**3** isomer (2.73 ppm). This isomer was assigned as the less stable *cis*-**3a**. Coupling constants of 12.21 and 7.32 Hz were found for H(2′) and H(3′), indicating the pseudoequatorial orientation of the methyl substituent at the stereogenic center (Table 1).

Prolonged irradiation[27] led to the establishment of a photostationary state consisting of all forms with the ratio of starting stable *cis*-**3**/less stable *trans*-**3a**/less stable *cis*-**3a**/stable *trans*-**3** of 19:41.5:29.5:10. The same photostationary state was achieved upon prolonged irradiation of a solution of stable *trans*-**3**. Monitoring the composition of the reaction mixture upon irradiation of *trans*-**3** by ^{1}H NMR

(27) It should be noted that irradiation times strongly depend on concentration and light sources used. The intrinsic photochemical *cis*−*trans* isomerization proceeds in a picosecond timescale. Zijlstra, R. W. J.; van Duijnen, P. T.; Feringa, B. L.; Steffen, T.; Duppen, K.; Wiersma, D. A. *J. Phys. Chem. A* **1997**, *101*, 9828–9836.

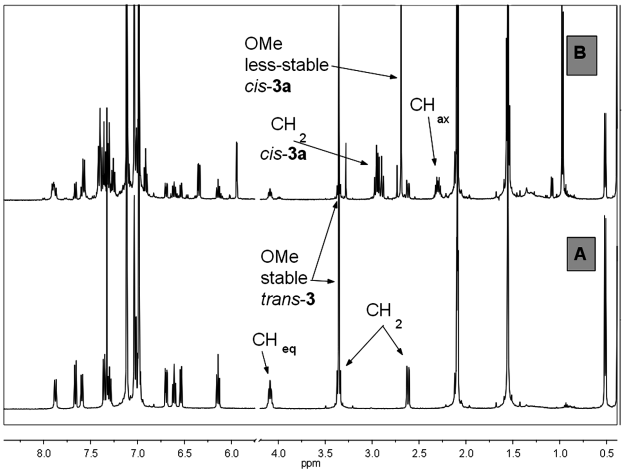

FIGURE 7. ^{1}H NMR spectra (toluene-d_8) of *trans*-**3** (A) before and (B) after irradiation at 355 nm (30 min).

SCHEME 3. Photochemical and Thermal Isomerization Process of *cis*-3 and *trans*-3[a]

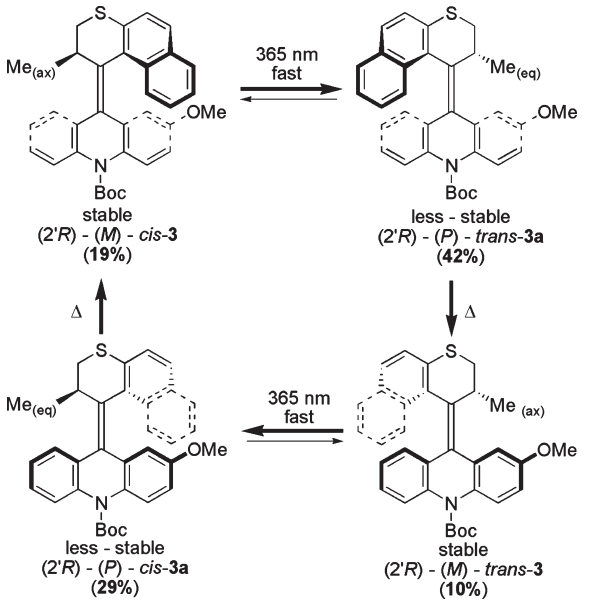

[a]Only (2′*R*) enantiomers are shown for clarity.

spectroscopy revealed a fast rise in concentration of less stable *cis*-**3a** at the onset of the isomerization processes. After approximately 20 min, a maximum amount of *cis*-**3a** was reached (Figures 5B and 7, Scheme 3), and its concentration then decreased due to formation of the other two isomers *cis*-**3** and *trans*-**3a**. The presence of distinct maxima (Figure 5A,B) for the initially formed less stable isomers in both photochemical reactions indicates that a multicomponent equilibrium involving at least four consequent switching processes occurs in these systems (Scheme 3). From the kinetic data shown in Figure 5A,B, it is evident that the fastest steps are isomerizations between *cis*-**3** and *trans*-**3a** and between *trans*-**3** and *cis*-**3a**, as the constant ratios of 1:2 and 1:3, respectively, are achieved readily ($t = 100$ min).

Thermodynamic parameters for the thermal conversion of *cis*-**3a** to *cis*-**3** and *trans*-**3a** to *trans*-**3** were determined by

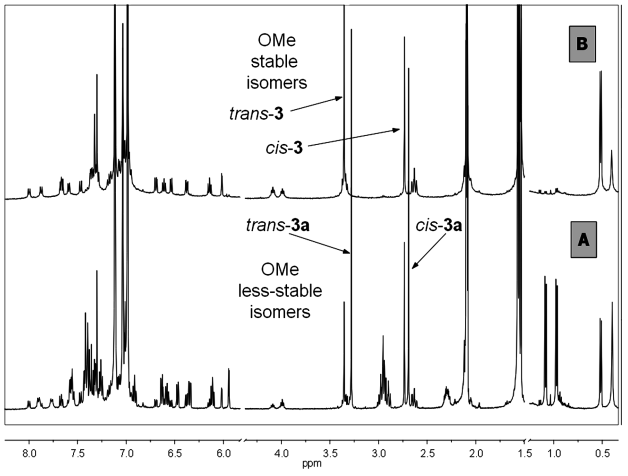

FIGURE 8. ^{1}H NMR spectra (toluene-d_8) of (A) the photostationary state achieved upon separate irradiation of both *cis*-**3** and *trans*-**3** and (B) the mixture of stable isomers after thermal isomerization.

^{1}H NMR spectroscopy by monitoring the decrease of integral intensities for the methyl substituents at the 2′-position and the increasing intensity of the signal at 0.51 ppm (Figure 8) in the range of 333.15−383.15 K.[28] Thus, for the conversion of *cis*-**3a** to *cis*-**3**, the following parameters were determined: $\Delta^{\ddagger}G^{\circ} = 107.5 \pm 0.2$ kJ·mol^{-1} ($\Delta^{\ddagger}H^{\circ} = 81.9 \pm 0.6$ kJ·mol^{-1}, $\Delta^{\ddagger}S^{\circ} = -87.9 \pm 0.9$ J·mol^{-1}·K^{-1}, $E_a = 84.8 \pm 0.1$ kJ·mol^{-1}, $A = (5.0 \pm 0.1) \times 10^8$ s^{-1}, $t_{1/2}$ (20 °C) = 454 ± 62 h, k (20 °C) = $(4.24 \pm 0.6) \times 10^{-7}$ s^{-1}). For the *trans*-**3a** to *trans*-**3** conversion, the results were $\Delta^{\ddagger}G^{\circ} = 106.7 \pm 0.2$ kJ·mol^{-1} ($\Delta^{\ddagger}H^{\circ} = 86.0 \pm 0.3$ kJ·mol^{-1}, $\Delta^{\ddagger}S^{\circ} = -71.4 \pm 0.9$ J·mol^{-1}·K^{-1}, $E_a = 97.8 \pm 0.2$ kJ·mol^{-1}, $A = (2.0 \pm 0.1) \times 10^{15}$ s^{-1}, $t_{1/2}$ (20 °C) = 323 ± 34 h, k (20 °C) = $(6.90 \pm 0.1) \times 10^{-7}$ s^{-1}). Considering these data, it is evident that *trans*-**3a** is thermally more labile than *cis*-**3a**, which might be attributed to the increased steric hindrance between the methoxy substituent on the stator and the naphthalene moiety of the rotor, while no significant thermal conversion occurs when irradiation is performed at room temperature. Despite this complex photochemical isomerization behavior among four isomers, these alkenes can still be considered molecular motors, albeit with less efficiency due to minor but nonignorable photoisomerization pathways. The fact that upon prolonged irradiation competing photochemical pathways appear is mainly due to the slow thermal isomerization from the unstable to the stable isomers.[19]

Synthesis of Molecular Motors 2, *cis*-10, and *trans*-10. As was described above, overcrowded alkenes containing an acridane-like lower stator part bearing N-substituents can act effectively as molecular rotary motors under normal conditions only if the conversion of less stable isomers into stable forms would dominate over competing photochemical switching processes. This goal can be achieved by strong acceleration of the thermally induced isomerization, which indeed dramatically increased in response to reduction of steric hindrance between the lower and the upper halves in the fjord region of the molecule.[29]

(28) See Supporting Information online.

(29) (a) Cnossen, A.; Pijper, D.; Kudernac, T.; Pollard, M. M.; Katsonis, N.; Feringa, B. L. *Chem.—Eur. J.* **2009**, *15*, 2768–2772. (b) Augulis, R.; Klok, M.; Feringa, B. L.; van Loosdrecht, P. H. M. *Phys. Status Solidi C* **2009**, *6*, 181–184.

SCHEME 4. Synthesis of Molecular Motors 2, *cis*-10, and *trans*-10[a]

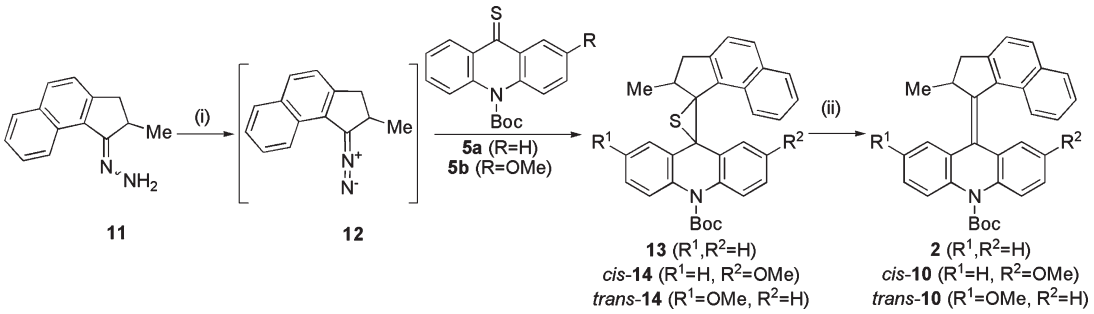

[a]Key: (i) $PhI(OCOCF_3)_2$, Me_2NCHO, −50 °C, 69−72%; (ii) $(4\text{-MeO-}C_6H_4)_3P$, toluene, reflux, 86−90%.

TABLE 2. Selected ^{1}H NMR data of 2, *cis*-10, and *trans*-10 in Chloroform-*d*

	chemical shift, ppm (coupling constants, Hz)				
compound	MeO	$Me_{(ax)}$	H(2′) (eq)	H(3′) (eq)	H(3′) (ax)
2		0.88 (6.84)	4.41 (6.35, 15.63)	3.67 (6.35, 15.63)	2.65 (15.63)
cis-**10**	2.91	0.88 (6.84)	4.42 (6.34, 15.63)	3.65 (6.34, 15.62)	2.67 (15.62)
trans-**10**	3.87	0.90 (6.83)	4.40 (6.34, 6.83)	3.07 (6.34, 15.63)	2.66 (15.63)

A 2-methyl-2,3-dihydro-1*H*-cyclopenta[*a*]naphthalene rotor was connected to the stators **5a** and **5b** described above, by an alternative diazo-thioketone coupling developed in our group.[30] Using this method, reaction of hydrazone **11** with bis(trifluoracetoxy)iodobenzene[31] at −50 °C in dimethylformamide provided diazo precursor **12** for the rotor, and subsequent addition of thioketone **5a** afforded episulfide **13** as a colorless solid in 72% yield (Scheme 4).

Desulfurization of **13** by heating at reflux in toluene solution in the presence of tris(4-methoxyphenyl)phosphine provided **2** with a symmetrical stator (Scheme 4). Similarly, a mixture of episulfides *cis*-**14** and *trans*-**14** (ratio of 2.3:1) was prepared from thioketone **5b**. Because complete separation of *trans*-**14** and *cis*-**14** was problematic, the subsequent desulfurization reaction was performed using the mixture, providing *trans*-**10** and *cis*-**10**. These isomers were separated by flash column chromatography (silica gel, *n*-pentane/ether = 10: 1) to yield pure *trans*-**10** (28%) as a white solid and *cis*-**10** (56%) as a yellow solid.

Alkenes **2**, *cis*-**10**, and *trans*-**10** were characterized by ^{1}H and ^{13}C NMR spectroscopy and HRMS. The assignment of the *trans* and *cis* geometry around the central double bond was based on by X-ray crystallographic analysis (vide infra). The chemical shifts of selected ^{1}H NMR absorptions can be found in Table 2. The signals of the methoxy substituents at the stator are found at 3.87 ppm (*trans*-**10**) and 2.91 ppm (*cis*-**10**). The difference in shielding by the naphthalene moiety of the rotor part in these compounds explains the shifts of the methoxy absorptions. Importantly, in order to demonstrate the unidirectional nature of the rotary process, enantioresolution of both (±)-*cis*-**10** and (±)-*trans*-**10** was achieved by preparative chiral HPLC (Chiralpak AD) under normal phase conditions using heptane/2-propanol = 99:1 as eluent at 50 °C. The absolute configuration of the second eluted enantiomer in both cases was assigned (2′*S*)-(*M*)-(*cis*/*trans*)-**10**, by comparison of the CD data with those of related compounds. Enantioresolution of (±)-**2** could not be achieved so far.

Stereochemistry of New Molecular Motors. The orientations of the methyl substituent at the 2′-position in the rotor part of **2**, *cis*-**10**, and *trans*-**10** were established by ^{1}H NMR spectroscopy. ^{1}H−^{1}H COSY spectra[28] of **2** indicated very weak coupling between H(2′) and one of the H(3′) protons (see Figure 9 for adopted numbering scheme). For this reason, direct determination of the coupling constants could not be performed. However, the coupling constant of the doublet at 2.65 ppm, assigned to one of the H(3′) protons, was found to be 1.65 Hz. It reduced to 1.42 Hz upon saturation of the H(2′) proton, suppressing the minor coupling. Spin simulation[32] using these data allowed the value of the coupling constant to be estimated at around 0.44 Hz. Thus, the dihedral angle between this H(3′) and the H(2′) protons should be expected to be close to 90°,[33] which is possible only in the case when H(2′) adopts a pseudoequatorial orientation. Therefore, an axial orientation of the methyl substituent is assumed. Similar parameters were obtained for *cis*-**2** and *trans*-**2** (Table 2).

In order to confirm the structure and to determine the orientation of the methyl substituent unequivocally, an X-ray structural analysis was performed. Sharp, white needles of racemic *cis*-**2** were obtained by slow diffusion of methanol into a saturated solution of *cis*-**2** in dichloromethane. The asymmetric unit of the monoclinic unit cell was found to contain two residues.[34] These residues are denoted residues 1 and 2 and differ in the absolute configuration at the stereogenic center. The structure in the solid state of *cis*-**2** (Figure 9a,b) was found to be comparable to that of the previously described motors. The length of the C(1′)−C(9)

(30) Wiel, T.; Matthijs, K. J.; Vicario, J.; Davey, S. G.; Meetsma, A.; Feringa, B. L. *Org. Biomol. Chem.* **2005**, *3*, 28–30.
(31) London, G. M.; Radhakrishna, A. S.; Almond, M. R.; Blodgett, J. K.; Boutin, B. H. *J. Org. Chem.* **1984**, *49*, 4272–4276.
(32) Incorporated in the standard Varian NMR software package Vnmr 6.1 C.
(33) Wu, A.; Cremer, D.; Auer, A. A.; Gauss, J. *J. Phys. Chem. A* **2002**, *106*, 657–667.
(34) The small differences between both residues can be ascribed to crystal packing effects.

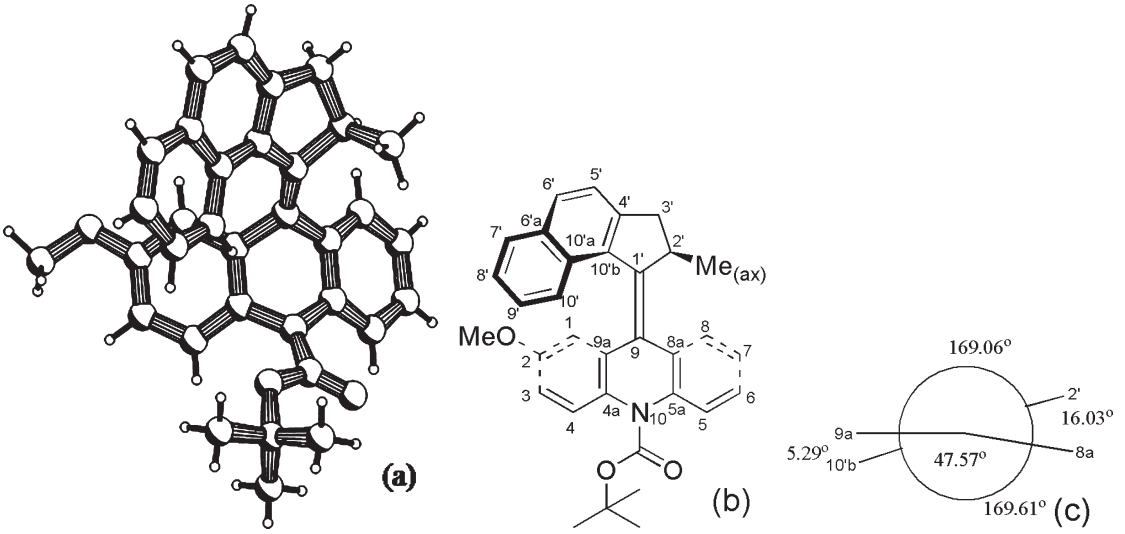

FIGURE 9. (a) PLUTO drawing and (b) chemical structure with adopted numbering scheme of racemic *cis*-**2** (one enantiomer shown; this structure does not express the absolute stereochemistry of the molecule); (c) conformation around the central double bond depicted as the Newman projection.

central double bond for both residues 1 and 2 was found to be 1.36 Å, which is relatively long compared to the value found for the earlier reported second-generation molecular motors with six-membered ring rotors.[10] The geometry around the central double bond can be characterized as follows (for all the values given, residue 1/residue 2): bond angles around central double bond C(9a)−C(9)−C(8a) = 109.94°/110.47°, C(9a)−C(9)−C(1′) = 124.88°/122.60°, C(8a)−(9)−C(1′) = 125.02°/126.91° (total angle around C(9) is 359.84°/359.98°), C(10b)−C(1′)−C(2′) = 105.65°/105.72°, C(10b)−C(1′)−C(9) = 129.45°/127.84°, C(9)−C(1′)−C(2′) = 124.71°/126.13° (total angle around C(2′) is 359.81°/359.69°); the dihedral angle between the naphthalene plane of the rotor and the central double bond C(10a)−C(10b)−C(1′)−C(9) = 30.54°/31.77°; dihedral angles between the arene moieties of the stator and the central double bond, C(1′)−C(9)−C(8a)−C(8) = −51.29°/−45.05°, C(1′)−C(9)−C(9a)−C(1) = 50.48°/44.04°; dihedral angles around central double bond C(10b)−C(1′)−C(9)−C(8a) = 169.61°/169.82°, C(2′)−C(1′)−C(9)−C(9a) = 169.06°/164.31° (average value is 169.34°/167.07°), C(2′)−C(1′)−C(9)−C(8a) = 16.03°/17.38°, C(10b)−C(1′)−C(9)−C(9a) = 5.29°/8.50° (average value is 10.66°/12.94°).

The central double bond is therefore considerably twisted, as is depicted schematically in the Newman projection in Figure 9c. The lower acridane part of the molecules adopts a folded structure (angle between both arene moieties: C(9a)−C(9)−C(8a) = 47.57°/C(4a)−N(10)−C(5a) = 51.32°) to diminish the steric strain around the central double bond and together with the twisted conformation of the cyclopentene ring of the upper part determines the helical shape of the entire molecule. From the X-ray data, it is evident that the methyl substituent attached to the stereogenic carbon atom has a pseudoaxial orientation. The torsion angles for C(9)−C(1′)−C(2′)−C(2′C) = −90.39°/−-93.30° in both residues are in agreement with those based on the ^{1}H NMR spectroscopic data.

Photochemical and Thermal Behavior of 2. Due to the presence of the five-membered ring in the upper half of **2**, a considerable reduction in the thermal stability of unstable

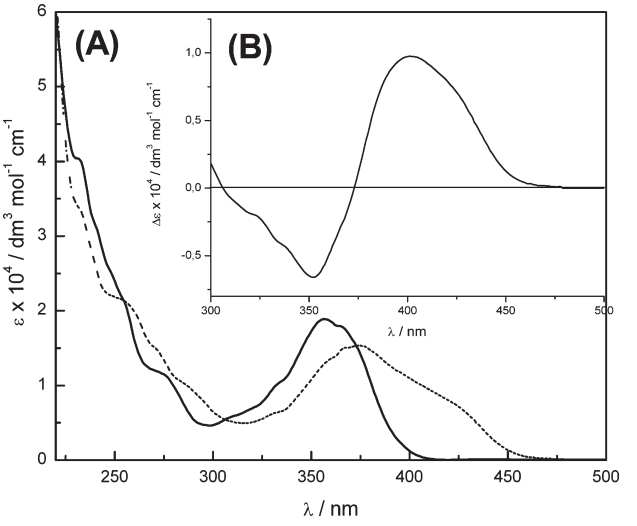

FIGURE 10. (A) UV/vis spectra at 115 K (*i*-pentane) of **2** (solid line) and the photostationary mixture of **2** and **2a** after irradiation with 355 nm light (dotted line) and (B) differential absorption spectrum of **2a** at 115 K.

isomer **2a** is expected relative to related compound **1a**.[24] Irradiation of a solution of racemic **2** in *i*-pentane at 115 K, followed by UV/vis spectroscopy (Figure 10a), resulted in the formation of a red-shifted maximum (λ_{max} = 371 nm) accompanied with the presence of clear isosbestic points,[28] similar to the case of the first-generation molecular motors.[35] The UV/vis spectrum of the photostationary mixture containing **2** and **2a** (Scheme 5) was completely restored within 60 s to that of the initial stable isomer by heating the solution to 130 K, indicative of the clean reverse thermal isomerization of **2a** to **2**.

As ^{1}H NMR spectroscopic determination of coupling constants for **2a** is challenging at these temperatures,

(35) Wiel, M. K. J.; van Delden, R. A.; Meetsma, A.; Feringa, B. L. *J. Am. Chem. Soc.* **2003**, *125*, 15076–15086.

SCHEME 5. Photochemical and Thermal Behavior of 2

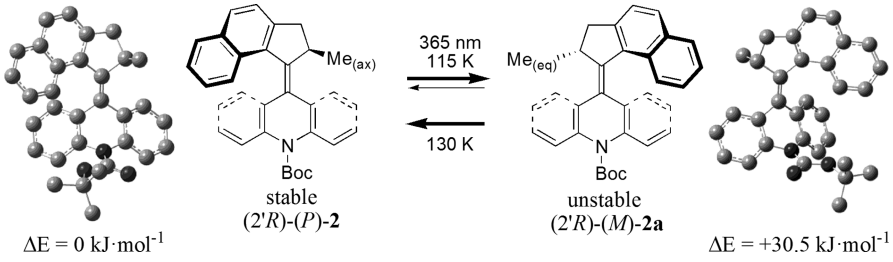

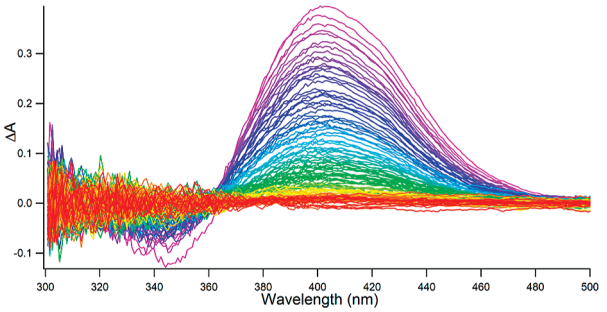

FIGURE 11. Transient absorption spectra (*n*-hexane) of **2a** at 20 °C generated with a nanosecond laser pulse of 355 nm.

DFT calculations[36] were performed to obtain information about the orientation of the methyl group at the stereogenic center, while at the same time providing information on the relative stabilities of the possible conformers of **2**. As shown in Scheme 5 for the case of the lowest energy isomer of **2**, the methyl substituent at the stereogenic center adopts a pseudoaxial orientation to prevent steric hindrance with the stator. The other isomer (**2a**), having a methyl group at the upper part in a pseudoequatorial orientation, is less stable. The energy difference caused by a strong twist of the central double bond between the lower energy isomer of **2** and the higher energy conformation **2a** was found to amount to +30.5 kJ·mol^{-1}, ensuring that the thermal equilibrium between **2a** and **2** lies quantitatively at the side of **2** at room temperatures.

A convenient way to study the thermal behavior of **2a** is to use time-resolved transient absorption differential spectroscopy. Using this technique, unstable isomer **2a** can be generated while following its fate in time, under ambient conditions.[37] Photoexcitation of a solution of **2** in *n*-hexane with a laser pulse of 355 nm at 20 °C resulted in the formation of a transient species[38] with a maximum absorption at 400 nm, which is close to the maximum observed by the cryogenic UV/vis experiment described above (Figures 10b and 11). In order to determine kinetic and thermodynamic parameters, the rate of disappearance of the absorption of transient **2a** was monitored at 400 nm over the temperature range of

SCHEME 6. Rotation Cycle of Ultrafast Nanomotor

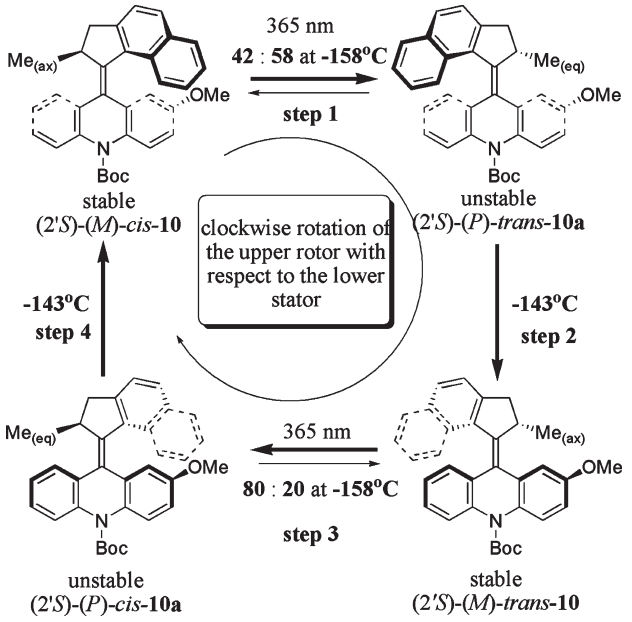

253.15−293.15 K: $\Delta^{\ddagger}G^{\circ} = 37.6 \pm 0.1$ kJ·mol^{-1} ($\Delta^{\ddagger}H^{\circ} = 35.2 \pm 0.7$ kJ·mol^{-1}, $\Delta^{\ddagger}S^{\circ} = -22.4 \pm 3.5$ J·mol^{-1}·K^{-1}, $E_a = 37.5 \pm 0.1$ kJ·mol^{-1}, $A = (5.7 \pm 0.3) \times 10^{12}$ s^{-1}, k (20 °C) = $(1.21 \pm 0.05) \times 10^{6}$ s^{-1}, $t_{1/2}$ (20 °C) = $(5.74 \pm 0.17) \times 10^{-7}$ s). The calculated half-life time of **2a** at 115 K ($t_{1/2}$ (115 K) = 2.29 ± 0.14 h) indicated that reverse thermal *cis*−*trans* isomerization can be neglected under these conditions.

Unidirectionality of Rotation of Molecular Motors (*cis*-10 and *trans*-10). To be able to identify the four distinct steps that define a full 360° rotary cycle of the rotor with respect to the stator as shown in Scheme 6, the photochemical behavior of overcrowded alkenes with methoxy-functionalized stator was studied by UV/vis spectroscopy.

During irradiation of a solution of *cis*-**10** in *i*-pentane at 115 K, continuous formation of a new species was observed by a red shift of the long wavelength absorption. The formation of a less stable isomer was also observed in the UV/vis spectra upon irradiation of *trans*-**10** under the same conditions. In both cases, increasing the temperature of the solution to 130 K resulted in the complete disappearance of the absorptions at 400 nm within 60 s (Figure 12, panels 1 and 2). Changes in the produced spectra compared to the UV/vis spectra of initial *cis*-**10** and *trans*-**10** obtained after this procedure reflect the alteration in composition of the sample solution with respect to the original solution, indicative of *cis*−*trans* isomerization. To prove the difference in photo-

(36) Frisch, M. J. *GaussView*, version 3; Gaussian, Inc.: Wallingford, CT, 2004.

(37) (a) Hviid, L.; Bouwman, W. G.; Paddon-Row, M. N.; van Ramesdonk, H. J.; Verhoeven, J. W.; Brouwer, A. M. *Photochem. Photobiol. Sci.* **2003**, *2*, 995–1001. (b) Brouwer, A. M.; Frochot, C.; Gatti, F. G.; Leigh, D. A.; Mottier, L.; Paolucci, F.; Roffia, S.; Wurpel, G. W. H. *Science* **2001**, *291*, 2124–2128.

(38) The absorption profile of the transient spectrum did not change both upon its generation using polar acetonitrile as a solvent and in oxygen free hexane, confirming that the transient species have a neutral and nonradical nature.

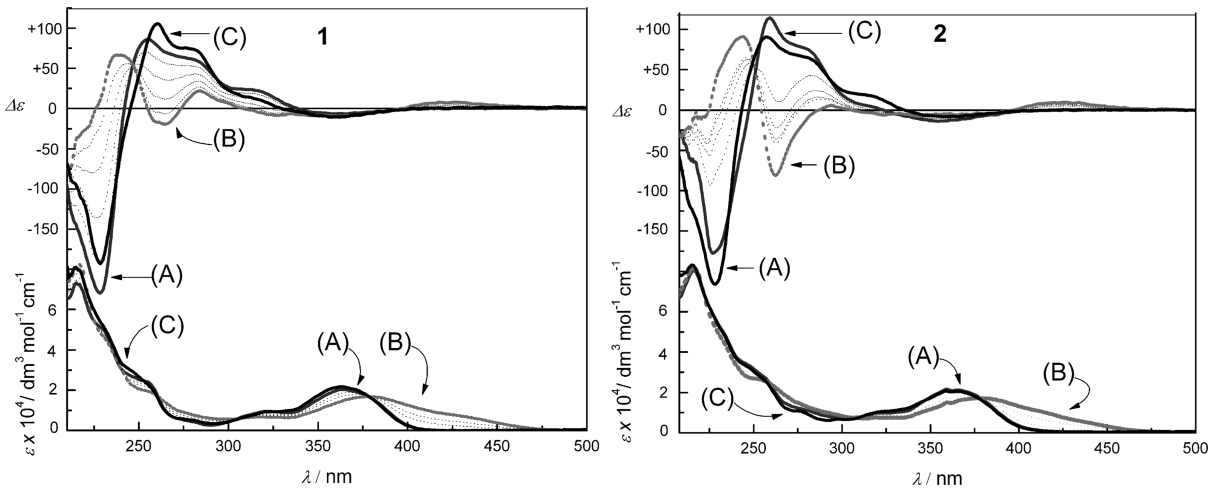

FIGURE 12. UV/vis and CD spectra of (2′*S*)-(*M*)-*cis*-**10** (1) and (2′*S*)-(*M*)-*trans*-**10** (2) and change in UV/vis and CD upon irradiation and the inversion of the sign of Cotton effects during irradiation in *i*-pentane at −115 K; (A) initial stable isomer, (B) at the photostationary state, (C) mixtures of (2′*S*)-(*M*)-*cis*-**10** (1) and (2′*S*)-(*M*)-*trans*-**10** after thermal conversions.

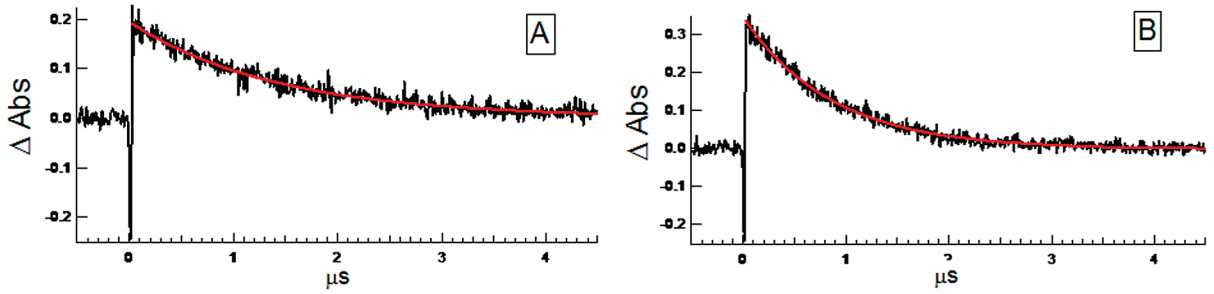

FIGURE 13. Experimental curves for the thermal conversion of transient (A) *cis*-**10a** and (B) *trans*-**10a** monitored at 410 nm in time at 295.15 K.

stationary states, the photochemical *trans*−*cis* and *cis*−*trans* isomerizations were also examined by CD spectroscopy using isolated enantiomers of *trans*-**10** and *cis*-**10** (Figure 12, panels 1 and 2). Irradiation of the solutions of the stable (2′*S*)-(*M*)-*trans*-**10** and (2′*S*)-(*M*)-*cis*-**10** isomers in *i*-pentane at 365 nm at 115 K over 5 min resulted in the formation of the unstable (2′*S*)-(*P*)-*cis*-**10a** and (2′*S*)-(*P*)-*trans*-**10a** isomers accompanied with a change in sign of the major CD absorptions. This is indicative of the *M* to *P* helix inversions of the molecules and difference in the photostationary states produced, which do not change after prolonged irradiation, confirming that no competing minor photoisomerizations, as observed in the case of *cis*- and *trans*-alkenes **3** (Scheme 3), occur. Furthermore, because several distinct isosbestic points were observed in both CD and UV/vis spectra, no degradation and/or side reactions occurred in these photochemical *trans*−*cis* and *cis*−*trans* isomerizations under these conditions. When the solutions were heated to 130 K for 10 min and cooled back to the initial temperature, complete conversion to the mixtures of (2′*S*)-(*M*)-*trans*-**10** and (2′*S*)-(*M*)-*cis*-**10** with different ratios in each case were observed, and the concomitant change in CD absorption confirmed the helix reversal, from *P* to *M* helicity, associated with these thermal interconversions. At the photoequilibria, ratios between (2′*S*)-(*M*)-*trans*-**10**/(2′*S*)-(*P*)-*cis*-**10a** of 20:80 (Scheme 6, step 3) and (2′*S*)-(*M*)-*cis*-**10**/(2′*S*)-(*P*)-*trans*-**10a** of 42:58 (Scheme 6, step 1) were determined.[39]

The kinetic and thermodynamic parameters for the thermal conversion of unstable isomers were measured using transient absorption spectroscopy. During thermal isomerization of unstable isomers, the decrease of transient absorption time traces was monitored at 410 nm after excitation of the respective solutions of *cis*-**10a** and *trans*-**10a** in *n*-hexane with 355 nm nanosecond laser pulse (Figure 13a,b) in the temperature range of 241.15−295.15 K. Thus, for unstable *cis*-**10a** isomer, the following data were determined: $\Delta^{\ddagger}G^{\circ} = 38.5 \pm 0.1$ kJ·mol^{-1} ($\Delta^{\ddagger}H^{\circ} = 28.7 \pm 0.7$ kJ·mol^{-1}, $\Delta^{\ddagger}S^{\circ} = -33.4 \pm 1.9$ J·mol^{-1}·K^{-1}, $E_a = 31.0 \pm 0.7$ kJ·mol^{-1}, $A = (3.1 \pm 0.1) \times 10^{11}$ s^{-1}, $t_{1/2}$ (20 °C) $= (8.25 \pm 0.11) \times 10^{-7}$ s, k (20 °C) $= (8.40 \pm 0.03) \times 10^{5}$ s^{-1}); and for unstable *trans*-**10a**: $\Delta^{\ddagger}G^{\circ} = 39.7 \pm 0.1$ kJ·mol^{-1} ($\Delta^{\ddagger}H^{\circ} = 25.3 \pm 0.8$ kJ·mol^{-1}, $\Delta^{\ddagger}S^{\circ} = -48.2 \pm 2.8$ J·mol^{-1}·K^{-1}, $E_a = 27.5 \pm 0.2$ kJ·mol^{-1}, $A = (4.2 \pm 0.1) \times 10^{10}$ s^{-1}, $t_{1/2}$ (20 °C) $= (1.32 \pm 0.13) \times 10^{-6}$ s, k (20 °C) $= (5.24 \pm 0.04) \times 10^{5}$ s^{-1}).

The distinct difference in photostationary states observed by CD spectroscopy (Scheme 6, steps 1 and 3) and the thermal stability of *trans*-**10a** and *cis*-**10a** together with *cis*−*trans* isomerization represent unequivocal evidence for the unidirectional rotation of the new ultrafast motor, which

(39) The ratios were obtained on the basis of analysis of solutions after thermal steps using analytical HPLC. They imply that no reverse *cis*−*trans* isomerizations occurred during the thermal conversions of unstable diastereoisomers into stable forms.

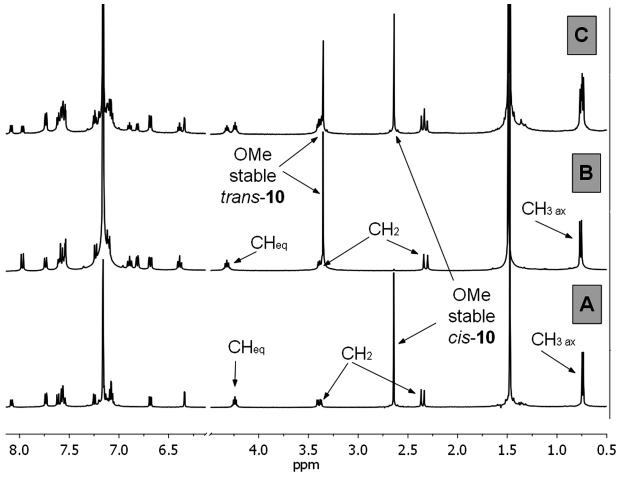

FIGURE 14. ^{1}H NMR spectra (benzene-d_6) of (A) *cis*-**10**, (B) *trans*-**10**, and (C) mixture of *cis*-**10** and *trans*-**10** in the motor working cycle governed by 365 nm at 295.15 K.

working cycle at 20 °C consists of (2′*S*)-(*M*)-*cis*-**10**/(2′*S*)-(*M*)-*trans*-**10** with a ratio of 67:33, as determined by ^{1}H NMR spectroscopy (Figure 14) and HPLC analysis.[28]

Scheme 6 summarizes the different isomers and the dynamic processes that are observed starting from (2′*S*)-(*M*)-*cis*-**10**. The experimental results show that the upper five-membered rotor undergoes a full 360° rotation around the central double bond in a clockwise sense relative to the lower acridane stator with a maximum possible rotational frequency of 0.5 MHz, strongly dependent on the temperature. Two photochemical conversions are both energetically uphill processes and generate the less stable isomers [(2′*S*)-(*M*)-*trans*-**10a** and (2′*S*)-(*P*)-*cis*-**10a**] with change of the helicity of the entire molecule. Subsequent thermal isomerization steps are energetically downhill processes generating stable isomers [(2′*S*)-(*M*)-*trans*-**10** and (2′*S*)-(*M*)-*cis*-**10**]. At the appropriate wavelength (365 ± 40 nm) and temperature (20 °C), a continuous unidirectional ultrafast rotation is induced in this molecular motor.

Conclusions. The thermal and photochemical behavior of two new types of molecular motors featuring N-Boc-protected nitrogen in the stator part, designed for attachment of appending groups, has been prepared. The working conditions for the second-generation motor with a six-membered ring rotor required high temperatures (above 373 K) for the thermal pathways to occur at considerable rate. The five-membered ring analogue displays a dramatic increase in the rate at which these steps occur, enhancing the speed of rotation by a factor of 10^{12} at 295.15 K. The new autonomous[40] nanomotor is, in principle, capable of performing its rotational cycle with 0.5 MHz frequency under optimal irradiation conditions.

Experimental Section

See the Supporting Information for general experimental methods, synthetic procedures, and characterization data for *tert*-butyl 9-oxoacridine-10(9*H*)-carboxylate **15a**, *tert*-butyl 2-methoxy-9-oxoacridine-10(9*H*)-carboxylate **15b**, **5a**, **5b**, and X-ray experimental data for *cis*-**10**.

A. Time-Resolved UV/Vis Spectroscopy. Nanosecond/OMA Setup. Excitation was produced by the third-harmonic of a Nd:YAG laser at 5 Hz (λ_{exc} = 355 nm, ~2.0 mJ pulse^{-1}, fwhm ~2 ns). The laser pulse was aligned to a slit (10 × 2 mm). The probe light source, a low-pressure xenon flash lamp at 10 Hz, which irradiated the sample through a 1 mm pinhole, about 1 mm from the edge of the cuvette was perpendicular to the laser pulse. The probe beam was split with a 50/50 quartz beam splitter into a reference beam (I_{ref}) and a signal beam (I). The signal beam passed through the sample, and both beams were guided through optical fibers to a spectrograph, which was coupled to a time-gated intensified CCD camera. The CCD camera recorded the spectra by opening the gate of the detector for 5 ns at different time delays after the laser pulse. The differences in light were corrected for both fibers by collecting the signal and the reference light without pumping the sample. When the sample was introduced, the transient absorption spectra were calculated by the logarithm of the intensity of the light aimed at the reference sample holder (I_0) divided by the intensity of light through the excited volume of the sample (I). The measurement of the difference in absorbance was calculated using the following formula:

$$\Delta A = A^t - A^0 = -\log\left(\frac{I^t}{I^t_{ref}}\right) + \log\left(\frac{I^0}{I^0_{ref}}\right) = \log\left(\frac{I^0 \times I^t_{ref}}{I^0_{ref} \times I^t}\right)$$

The laser, flash lamp, and CCD camera were synchronized with two pulse generators: a programmable pulse generator model and a pulse/delay generator, both controlled by a computer. Absorption spectra at different times after excitation were obtained with a time resolution of ~5 ns by varying the delay time between the laser pulse and the opening of the gate of the detector.

B. Monochromatic Wavelength Setup. The single wavelength setup used the same laser pulsing the sample (~6 mJ pulse^{-1}). The probe light, however, was provided by a Xe lamp with lamp housing LAX 1450 and a SVX1450 power supply. The probe light was led into a monochromator and detected by a GaAs photomultiplier connected to a digital oscilloscope with a resolution of 50 ns. The monochromator was set at 410 nm.

C. Compound Syntheses

1. *tert*-Butyl 2″-methyl-2″,3″-dihydro-10*H*-dispiro[acridine-9,2′-thiirane-3′,1″-benzo[*f*]thiochromene]-10-carboxylate (8). A mixture of 2-methyl-2,3-dihydro-1*H*-benzo[*f*]thiochromen-1-one hydrazone **4** (684 mg, 2.83 mmol) and $MgSO_4$ (2.00 g) in dichloromethane (40 mL) was cooled to 0 °C, and activated MnO_2 (2.50 g, 28.8 mmol) was added in one portion. The mixture was stirred at 0 °C for 2.5 h in the absence of light. The deep red solution of diazo compound **7** was quickly filtered through a plug of cotton into the ice-cooled collecting flask, and the remaining residue was washed with cold dichloromethane. Thioketone **5a** (586 mg, 1.88 mmol) was added slowly portionwise to the resulted solution until the evolution of nitrogen ceased. After stirring at room temperature for 1 h and removal of the solvent under reduced pressure, the crude product was purified by flash chromatography (SiO_2, *n*-pentane/ether = 10:1). Subsequent recrystallization from ethanol (60 mL) afforded pure **8** (660 mg, 1.26 mmol, 67%) as a white powder: mp 136−139 °C (sealed capillary); ^{1}H NMR (300 MHz, $CDCl_3$) δ = 1.24−1.27 (d, J = 6.96 Hz, 3H), 1.65 (s, 9H), 2.19−2.26 (dd, J = 7.68, 12.09 Hz, 1H), 2.68−2.75 (dd, J = 8.79, 12.09 Hz, 1H), 2.83−2.96 (ddq, J = 6.96, 7.68, 8.79 Hz, 1H), 6.24−6.29 (t, J = 7.69 Hz, 1H), 6.41−6.44 (dd, J = 1.10, 8.60 Hz, 1H), 6.80−6.86 (dt, J = 1.10, 8.79 Hz, 1H), 7.00−7.03 (d, J = 8.42 Hz, 1H), 7.21−7.26 (m, 1H), 7.33−7.42 (m, 4H), 7.52−7.57 (t, J = 7.69 Hz, 1H), 7.66−7.69 (d, J = 8.05 Hz, 1H), 7.79−7.82 (d, J = 8.05 Hz, 1H),

(40) Balzani, V.; Clemente-Leon, M.; Credi, A.; Ferrer, B.; Venturi, M.; Flood, A. H.; Stoddart, J. F. *Proc. Natl. Acad. Sci. U.S.A.* **2006**, *103*, 1178–1183.

7.87−7.84 (d, J = 8.05 Hz, 1H), 8.75−8.78 (d, J = 8.79 Hz, 1H); ^{13}C NMR (100 MHz, $CDCl_3$) δ = 21.6 (CH_3), 28.64 (CH_3), 36.7 (CH_2), 42.4 (CH), 59.6 (C−S), 65.4 (C−S), 81.9 (C−O), 123.292 (CH), 123.392 (CH), 124.3 (CH), 124.4 (CH), 124.5 (CH), 125.4 (CH), 125.4 (CH), 125.7 (CH), 126.2 (CH), 127.0 (CH), 127.0 (CH), 127.2 (CH), 128.4 (CH), 129.5 (CH), 129.8 (C), 130.4 (C), 130.4 (C), 1321.3 (C), 134.4 (C), 138.9 (C), 140.4 (C), 140.9 (C), 152.4 (C=O); m/z (EI, %) = 523 (M^+, 94.9), 467 (64.4), 422 (M^+ − Boc + H, 77.4), 211 (66.7), 57 (^{t}Bu$^+$, 100); HRMS (EI) calcd for $C_{32}H_{29}NO_2S_2$ 523.16395, found 523.16126.

2. *tert*-Butyl 9-(2-methyl-2,3-dihydro-1*H*-benzo[*f*]thiochromen-1-ylidene)acridine-10(9*H*)-carboxylate (1). A solution of episulfide **8** (645 mg, 1.23 mmol) was heated at reflux for 8 h in toluene (100 mL) in the presence of tris(4-methoxyphenyl)-phosphine (867 mg, 2.46 mmol). The reaction mixture was cooled to 60 °C and after addition of methyl iodide (2.00 mL) was stirred at this temperature for an additional 4 h. The white precipitate was filtered off, and removal of the solvent from the filtrate under reduced pressure followed by flash chromatography (SiO_2, *n*-pentane/ether = 10:1) and recrystallization from methanol (50 mL) afforded **1** (514 mg, 1.05 mmol, 85%) as a white solid: mp 288−292 °C (sealed capillary); ^{1}H NMR (500 MHz, $CDCl_3$) δ = 0.82−0.83 (d, J = 6.84 Hz, 3H), 1.68 (s, 9H), 3.18−3.21 (dd, J = 2.44, 11.23 Hz, 1H), 3.76−3.79 (dd, J = 6.35, 11.23 Hz, 1H), 4.22−4.27 (ddq, J = 2.44, 6.35, 6.84 Hz, 1H), 6.25−6.27 (d, J = 7.82 Hz, 1H), 6.32−6.35 (t, J = 7.81 Hz, 1H), 6.80−6.84 (t, J = 6.83 Hz, 1H), 7.01−7.04 (t, J = 7.32 Hz, 1H), 7.11−7.13 (t, J = 8.30 Hz, 1H), 7.26−7.38 (m, 4H), 7.44−7.46 (d, J = 8.30 Hz, 1H), 7.52−7.54 (d, J = 7.82 Hz, 1H), 7.58−7.59 (d, J = 7.32 Hz, 1H), 7.62−7.64 (d, J = 8.79 Hz, 1H), 7.87−7.89 (d, J = 8.30 Hz, 1H); ^{13}C NMR (100 MHz, $CDCl_3$) δ = 18.5 (CH_3), 28.4 (CH_3), 30.9 (CH), 37.0 (CH_2), 82.0 (C−O), 123.8 (CH), 124.1 (CH), 124.2 (CH), 124.3 (CH), 124.8 (CH), 125.2 (CH+CH), 125.8 (CH), 125.9 (CH), 126.0 (CH), 126.7 (CH), 127.0 (CH), 127.6 (CH), 127.7 (CH), 127.8 (C), 130.4 (C), 130.4 (C), 131.4 (C), 133.5 (C), 134.7 (C), 134.8 (C), 135.1 (C), 138.0 (C), 139.3 (C), 152.3 (C=O); m/z (EI, %) = 491 (M^+, 53.6), 435 (100), 390 (M^+ − Boc + H, 42.4), 57 (^{t}Bu$^+$, 48.9); HRMS (EI) calcd for $C_{32}H_{29}NO_2S$ 491.19189, found 491.19358. Anal. Calcd for $C_{32}H_{29}NO_2S$: C, 77.92; H, 6.04; N, 2.85; S, 6.46. Found: C, 78.03; H, 6.05; N, 2.85; S, 6.49.

(2′*R*)-(*M*)-**1**: UV/vis (*n*-hexane, 25 °C, λ ($\varepsilon \times 10^4$), nm) 222 (4.33), 260 (2.93), 325 (0.94), 361 sh (0.36); CD (*n*-hexane, 25 °C, λ ($\Delta\varepsilon$), nm) 222 (−91.8), 253 (−26.03), 275 (+73.2). 350 (−13.0).

3. Mixture of (*Z*)- and (*E*)-*tert*-Butyl 2-methoxy-2″-methyl-2″,3″-dihydro-10*H*-dispiro[acridine-9,2′-thiirane-3′,1″-benzo[*f*]-thiochromene]-10-carboxylate (*cis*-9 and *trans*-9). These compounds were prepared according to the procedure described for **8** starting from 2-methyl-2,3-dihydro-1*H*-benzo[*f*]thiochromen-1-one hydrazone **3** (650 mg, 2.68 mmol) and activated MnO_2 (2.50 g, 28.8 mmol). *tert*-Butyl 2-methoxy-9-thioxoacridine-10(9*H*)-carboxylate **5b** (426 mg, 1.25 mmol) was further introduced to react with preformed diazonium compound **7**. A mixture of *cis*-**9**/*trans*-**9** with a ratio of 1.74:1 was obtained as a white powder (478 mg, 0.86 mmol, 69%) and used for the next step. Additional chromatography (SiO_2, *n*-pentane/ether = 10:1) provided each isomer (96% purity by ^{1}H NMR), but complete separation of *trans*-**9** and *cis*-**9** could not be accomplished. *trans*-**9** (R_f = 0.3): ^{1}H NMR (500 MHz, $CDCl_3$) δ = 1.25−1.26 (d, J = 6.84 Hz, 3H), 1.64 (s, 9H), 2.22−2.26 (dd, J = 7.81, 12.70 Hz, 1H), 2.74−2.78 (dd, J = 8.79, 12.70 Hz, 1H), 2.92−3.00 (ddq, J = 6.84, 7.81, 8.79 Hz, 1H), 3.87 (s, 3H), 6.26−6.23 (t, J = 8.30 Hz, 1H), 6.39−6.41 (d, J = 8.30 Hz, 1H), 6.81−6.84 (t, J = 8.79 Hz, 1H), 6.90−6.92 (dd, J = 2.93, 8.79 Hz, 1H), 7.00−7.02 (d, J = 8.30 Hz, 1H), 7.35−7.41 (m, 4H), 7.52−7.56 (t, J = 7.81 Hz, 1H), 7.66−7.68 (d, J = 7.81 Hz, 1H), 7.75−7.77 (d, J = 8.79 Hz, 1H), 8.74−8.75 (d, J = 8.79 Hz, 1H); ^{13}C NMR (100 MHz, $CDCl_3$) δ = 21.6 (CH_3), 28.7 (CH_3), 36.7 (CH_2), 42.4 (CH), 55.6 (OCH_3), 59.7 (C−S), 65.4 (C−S), 81.7 (C−O), 112.5 (CH), 114.6 (CH), 123.2 (CH), 123.2 (CH), 124.4 (CH), 124.5 (CH), 125.4 (CH), 125.7 (CH), 126.1 (CH), 126.5 (CH), 127.0 (CH), 127.2 (CH), 128.4 (CH), 129.6 (C), 130.3 (C), 131.9 (C), 132.3 (C), 133.9 (C), 134.4 (C), 139.1 (C), 140.9 (C), 152.5 (C), 156.2 (C=O); HRMS (EI) calcd for $C_{33}H_{31}NO_3S_2$ 553.17451, found 553.17489. *cis*-**9** (R_f = 0.29): ^{1}H NMR (500 MHz, $CDCl_3$) δ = 1.27−1.28 (d, J = 6.97 Hz, 3H), 1.63 (s, 9H), 2.21−2.27 (dd, J = 8.06, 12.46 Hz, 1H), 2.71 (s, 3H), 2.69−2.74 (dd, J = 8.80, 12.46 Hz, 1H), 2.85−2.94 (ddq, J = 6.97, 8.06, 8.80 Hz, 1H), 5.98−5.99 (d, J = 2.93 Hz, 1H), 6.37−6.40 (dd, J = 2.93, 8.80 Hz, 1H), 7.04−7.06 (d, J = 8.07 Hz, 1H), 7.25−7.21 (m, 2H), 7.40−7.33 (m, 3H), 7.51−7.55 (t, J = 6.60 Hz, 1H), 7.68−7.70 (d, J = 7.70 Hz, 1H), 7.78−7.80 (d, J = 7.70 Hz, 1H), 7.85−7.87 (d, J = 8.07 Hz, 1H), 8.78−8.80 (d, J = 8.80 Hz, 1H); ^{13}C NMR (100 MHz, $CDCl_3$) δ = 21.7 (CH_3), 28.6 (CH_3), 36.8 (CH_2), 42.4 (CH), 54.1 (OCH_3), 60.0 (C−S), 65.4 (C−S), 81.7 (C−O), 109.4 (CH), 114.3 (CH), 132.3 (CH), 124.2 (CH), 124.5 (CH), 125.4 (CH), 125.4 (CH), 125.6 (CH), 126.3 (CH), 127.0 (CH), 127.1 (CH), 128.5 (CH), 129.5 (CH), 130.0 (C), 130.4 (C), 130.8 (C), 132.2 (C), 132.4 (C), 134.5 (C), 140.7 (C), 141.3 (C), 152.5 (C), 155.2 (C=O); m/z (EI, %) = 553 (M^+, 69.9), 497 (51.4), 452 (M^+ − Boc + H, 77.4), 57 (^{t}Bu$^+$, 100); HRMS (EI) calcd for $C_{33}H_{31}NO_3S_2$ 553.17451, found 553.17498.

4. (9*Z*)- and (9*E*)-*tert*-Butyl 2-methoxy-9-(2-methyl-2,3-dihydro-1*H*-benzo[*f*]thiochromen-1-ylidene) acridine-10(9*H*)-carboxylate (*cis*-3 and *trans*-3). A solution of a mixture of *cis*-**9** and *trans*-**9** (151 mg, 0.27 mmol) and tris(4-methoxyphenyl)-phosphine (191 mg, 0.54 mmol) in toluene (25 mL) was heated at reflux for 8 h. The reaction mixture was cooled to 60 °C and after addition of methyl iodide (4.00 mL) was stirred at this temperature for an additional 4 h. The white precipitate was filtered off, and the filtrate was concentrated under reduced pressure. Alkenes *cis*-**3** and *trans*-**3** were obtained after careful column chromatography (SiO_2, *n*-pentane/ether = 10:1). c*is*-**3** (R_f = 0.5, 71 mg, 0.13 mmol, 50%) was obtained as white solid after recrystallization from ethanol (50 mL): mp 272−276 °C (sealed capillary); ^{1}H NMR (500 MHz, $CDCl_3$) δ = 0.84−0.85 (d, J = 6.84 Hz, 3H), 1.67 (s, 9H), 2.99 (s, 3H), 3.18−3.20 (dd, J = 2.45, 11.23 Hz, 1H), 3.76−3.79 (dd, J = 6.83, 11.23 Hz, 1H), 4.21−4.27 (ddq, J = 2.45, 6.83, 6.84 Hz, 1H), 5.76−5.77 (d, J = 2.93 Hz, 1H), 6.36−6.38 (ddd, J = 1.46, 6.83, 9.77 Hz, 1H), 7.14−7.17 (ddd, J = 1.46, 6.83, 9.28 Hz, 1H), 7.25−7.28 (m, 1H), 7.31−7.38 (m, 4H), 7.52−7.53 (dd, J = 1.46, 7.81 Hz, 1H), 7.59−7.60 (d, J = 8.30 Hz, 1H), 7.62−7.63 (d, J = 8.30 Hz, 1H), 7.85−7.87 (dd, J = 1.46, 8.30 Hz, 1H); ^{13}C NMR (125 MHz, $CDCl_3$) δ = 18.6 (CH_3), 28.5 (CH_3), 31.0 (CH), 37.1 (CH_2), 54.9 (OCH_3), 81.8 (C−O), 110.1 (CH), 113.9 (CH), 124.1 (CH), 124.5 (CH), 124.7 (CH), 125.2 (CH), 125.2 (CH), 125.2 (CH), 125.9 (CH), 126.1 (CH), 126.8 (CH), 127.5 (CH), 127.6 (CH), 127.9 (C), 130.5 (C), 130.7 (C), 131.5 (C), 131.5 (C), 133.2 (C), 134.7 (C), 134.8 (C), 135.9 (C), 139.6 (C), 152.5 (C), 155.7 (C=O); HRMS (EI) calcd for $C_{33}H_{31}NO_3S$ 521.20245, found 521.20310. Anal. Calcd for $C_{33}H_{31}NO_3S$: C, 75.49; H, 5.96; N, 2.66; S, 6.06. Found: C, 75.44; H, 5.96; N, 2.69; S, 6.03. *trans*-**3** (R_f = 0.46, 52 mg, 0.1 mmol, 37%) was obtained as white solid after recrystallization from ethanol (50 mL): mp 292−296 °C (sealed capillary); ^{1}H NMR (300 MHz, $CDCl_3$) δ = 0.82−0.83 (d, J = 6.84 Hz, 3H), 1.67 (s, 9H), 3.18−3.21 (dd, J = 2.44, 11.23 Hz, 1H), 3.74−3.78 (dd, J = 6.84, 11.23 Hz, 1H), 3.87 (s, 3H), 4.27−4.32 (ddq, J = 2.44, 6.84, 6.84 Hz, 1H), 6.24−6.25 (dd, J = 1.46, 7.81 Hz, 1H), 6.30−6.33 (dd, J = 0.98, 9.70 Hz, 1H), 6.79−6.82 (ddd, J = 1.46, 6.83, 9.26 Hz, 1H), 6.88−6.91 (dd, J = 2.45, 9.28 Hz, 1H), 7.01−7.04 (ddd, J = 0.98, 6.84, 8.56 Hz, 1H), 7.05−7.06 (d, J = 2.45 Hz, 1H), 7.11−7.14 (dd, J = 0.98, 7.81, 8.56 Hz, 1H), 7.28−7.29 (d, J = 8.30 Hz, 1H), 7.36−7.37 (d, J = 8.30 Hz, 1H),

7.42−7.43 (d, J = 7.81 Hz, 1H), 7.57−7.59 (d, J = 8.30 Hz, 1H), 7.61−7.63 (d, J = 8.30 Hz, 1H), 8.76−8.78 (d, J = 9.28 Hz, 1H); ^{13}C NMR (100 MHz, $CDCl_3$) δ = 18.5 (CH_3), 28.5 (CH_3), 31.0 (CH), 37.0 (CH_2), 55.7 (OCH_3), 81.8 (C−O), 111.6 (CH), 111.8 (CH), 123.7 (CH), 124.1 (CH), 124.2 (CH), 124.3 (CH), 125.2 (CH), 125.8 (CH), 126.0 (CH+CH), 127.1 (CH), 127.6 (CH), 127.7 (CH), 127.9 (C), 130.4 (C), 130.4 (C), 131.4 (C), 132.8 (C), 134.60 (C), 134.7 (C), 135.0 (C+C), 138.3 (C), 152.5 (C), 156.5 (C═O); m/z (EI, %) = 521 (M^+, 44.8), 465 (100), 420 (M^+ − Boc + H, 47.7), 57 (^{t}Bu$^+$, 79.7); HRMS (EI) calcd for $C_{33}H_{31}NO_3S$ 521.20245, found 521.20370. Anal. Calcd for $C_{33}H_{31}NO_3S$: C, 75.49; H, 5.96; N, 2.66; S, 6.06. Found: C, 75.42; H, 5.95; N, 2.69; S, 6.03.

5. *tert*-Butyl 2″-methyl-2″,3″-dihydro-10*H*-dispiro[acridine-9,2′-thiirane-3′,1″-cyclopenta-[*a*]naphthalene]-10-carboxylate (13). A solution of 2-methyl-2,3-dihydro-1*H*-cyclopenta[*a*]-naphthalen-1-one hydrazone **11** (210 mg, 1 mmol) in DMF (20 mL) was cooled to −50 °C, and [bis(trifluoroacetoxy)-iodo]benzene (398 mg, 1 mmol) was added. After stirring for 10 s, *tert*-butyl 9-thioxoacridine-10(9*H*)-carboxylate **5a** (156 mg, 0.5 mmol) was added, and temperature of the mixture was allowed to reach a room temperature gradually. The mixture was poured into water (200 mL) and extracted with ether (2 × 100 mL). The combined organic layers were washed with brine and dried (Na_2SO_4). The organic volatiles were removed under reduced pressure to provide an orange oil which was purified by flash chromatography (SiO_2, *n*-pentane/ether = 10:1). Subsequent concentration of combined fractions (R_f = 0.4−0.6) and recrystallization of the yellow residue from ethanol (30 mL) afforded pure **13** (177 mg, 0.36 mmol, 72%) as a white powder: mp 255−258 °C (sealed capillary); ^{1}H NMR (500 MHz, $CDCl_3$) δ = 1.10−1.11 (d, J = 6.84 Hz, 3H), 1.46 (s, 9H), 1.83−1.88 (dq, J = 6.35, 6.84 Hz, 1H), 2.30−2.22 (d, J = 15.63 Hz, 1H), 2.99−3.03 (dd, J = 6.35, 15.63 Hz, 1H), 6.71−6.74 (dt, J = 0.97, 7.81 Hz, 1H), 6.81−6.84 (dt, J = 1.47, 7.81 Hz, 1H), 7.14−7.16 (d, J = 7.81 Hz, 1H), 7.17−7.19 (dd, J = 0.97, 7.81 Hz, 1H), 7.20−7.24 (m, 2H), 7.28−7.32 (m, 2H), 7.52−7.59 (m, 3H), 7.68−7.70 (dd, J = 0.97, 7.81 Hz, 1H), 7.72−7.73 (dd, J = 1.46, 7.81 Hz, 1H), 9.18−9.20 (d, J = 8.78 Hz, 1H); ^{13}C NMR (125 MHz, $CDCl_3$) δ = 20.9 (CH_3), 28.2 (CH_3), 36.7 (CH_2), 41.6 (CH), 57.9 (C−S), 71.0 (C−S), 81.8 (C−O), 123.4 (CH), 123.6 (CH), 123.8 (CH), 124.1 (CH), 124.2 (CH), 124.3 (CH), 124.6 (CH), 124.8 (CH), 126.6 (CH), 126.8 (CH), 127.0 (CH), 127.9 (CH), 128.9 (CH), 129.0 (CH), 131.3 (C), 131.5 (C), 131.5 (C), 132.9 (C), 135.4 (C), 139.8 (C), 140.1 (C), 141.5 (C), 151.5 (C═O); m/z (EI, %) = 491 (M^+, 57.6), 435 (100), 390 (M^+ − Boc + H, 79.2), 57 (^{t}Bu$^+$, 93.3); HRMS (EI) calcd for $C_{32}H_{29}NO_2S$ 491.19189, found 491.19417.

6. *tert*-Butyl 9-(2-methyl-2,3-dihydro-1*H*-cyclopenta[*a*]naphthalen-1-ylidene)acridine-10(9*H*)-carboxylate (2). This compound was prepared according to the procedure described for **1** starting from *tert*-butyl 2″-methyl 2″,3″-dihydro-10*H*-dispiro-[acridine-9,2′-thiirane-3′,1″-cyclopenta[*a*]naphthalene]-10-carboxylate **13** (170 mg, 0.35 mmol) and tris(4-methoxyphenyl)-phosphine (147 mg, 0.42 mmol). Treatment of the final reaction mixture with methyl iodide (2.00 mL) followed by flash chromatography (SiO_2, *n*-pentane/ether = 10:1) and subsequent recrystallization from ethanol (20 mL) afforded pure **2** (138 mg, 0.30 mmol, 86%) as a slightly yellowish powder: mp 213−217 °C (sealed capillary); ^{1}H NMR (500 MHz, $CDCl_3$) δ = 0.87−0.88 (d, J = 6.84 Hz, 3H), 1.61 (s, 9H), 2.64−2.67 (d, J = 15.63 Hz, 1H), 3.65−3.69 (dd, J = 6.35, 15.63 Hz, 1H), 4.38−4.44 (dq, J = 6.35, 6.84 Hz, 1H), 6.53−6.56 (t, J = 7.81 Hz, 1H), 6.61−6.63 (d, J = 7.81 Hz, 1H), 6.86−6.89 (t, J = 7.81 Hz, 1H), 7.03−7.06 (t, J = 7.83 Hz, 1H), 7.07−7.09 (d, J = 8.30 Hz, 1H), 7.18−7.21 (t, J = 7.81 Hz, 1H), 7.23−7.30 (m, 2H), 7.44−7.45 (d, J = 8.30 Hz, 1H), 7.60−7.62 (d, J = 7.82 Hz, 1H), 7.71−7.75 (m, 2H), 7.82−7.83 (d, J = 8.30 Hz, 1H), 7.88−7.89 (d, J = 7.82 Hz, 1H); ^{13}C NMR (125 MHz, $CDCl_3$) δ = 19.0 (CH_3), 28.4 (CH_3), 37.9 (CH), 40.3 (CH_2), 81.7 (C−O), 123.8 (CH), 124.0 (C), 124.1 (CH), 124.6 (CH), 125.0 (CH), 125.2 (CH), 125.3 (CH), 125.4 (CH), 125.9 (CH), 126.0 (CH), 126.6 (CH), 127.1 (CH), 127.9 (CH), 128.6 (C), 130.0 (CH), 133.1 (C), 135.6 (C), 135.7 (C), 137.3 (C), 138.9 (C), 139.1 (C), 145.0 (C), 146.2 (C), 152.4 (C═O); m/z (EI, %) = 459 (M^+, 37.7), 403 (100), 358 (M^+ − Boc + H, 82.5), 57 (^{t}Bu$^+$, 63.8); UV/vis (*i*-pentane, 25 °C, λ ($\varepsilon \times 10^4$), nm) 232 (6.10), 277 (1.67), 358 (2.85); HRMS (EI) calcd for $C_{32}H_{29}NO_2$ 459.21981, found 459.22135. Anal. Calcd for $C_{32}H_{29}NO_2$: C, 83.63; H, 6.36; N, 3.04. Found: C, 83.65; H, 6.35; N, 3.05.

7. Mixture of (*Z*)- and (*E*)-*tert*-Butyl 2-methoxy-2″-methyl-2″,3″-dihydro-10*H*-dispiro[acridine-9,2′-thiirane-3′,1″-cyclopenta[*a*]naphthalene]-10-carboxylate (*cis*-14 and *trans*-14). These compounds were prepared according to the procedure described for **13** starting from 2-methyl-2,3-dihydro-1*H*-cyclopenta-[*a*]naphthalen-1-one hydrazone **11** (420 mg, 2 mmol), [bis(trifluoroacetoxy)iodo]benzene (796 mg, 2 mmol), and *tert*-butyl 2-methoxy-9-thioxoacridine-10(9*H*)-carboxylate **5b** (342 mg, 1 mmol). The mixture of *cis*-**14** and *trans*-**14** isomers of 2.3:1 ratio was obtained as a yellowish powder (360 mg, 0.69 mmol 69%). Additional chromatography (SiO_2, *n*-pentane/ether = 10:1) provided each isomer (96% purity by ^{1}H NMR), but complete separation of *trans*-**14** and *cis*-**14** could not be accomplished. *cis*-**14** (R_f = 0.29): ^{1}H NMR (500 MHz, $CDCl_3$) δ = 1.09−1.11 (d, J = 6.84 Hz, 3H), 1.45 (s, 9H), 1.81−1.87 (dq, J = 6.84, 6.35 Hz, 1H), 2.29−2.32 (d, J = 15.62 Hz, 1H), 2.99−3.03 (dd, J = 6.35, 15,62 Hz, 1H), 3.71 (s, 3H), 6.35−6.37 (dd, J = 2.92, 8.78 Hz, 1H), 7.08−7.10 (d, J = 8.78 Hz, 1H), 7.15−7.16 (d, J = 8.30 Hz, 1H), 7.19−7.32 (m, 6H), 7.54−7.59 (m, 3H), 7.66−7.68 (d, J = 7.82 Hz, 1H), 9.23−9.25 (d, J = 8.79 Hz, 1H); ^{13}C NMR (100 MHz, $CDCl_3$) δ = 20.9 (CH_3), 26.3 (CH_3), 36.7 (CH_2), 41.6 (CH), 55.4 (OCH_3), 58.1 (C−S), 71.2 (C−S), 80.2 (C−O), 113.2 (CH), 113.3 (CH), 123.7 (CH), 124.1 (CH), 124.3 (CH), 124.4 (CH), 124.4 (CH), 124.6 (CH), 124.7 (CH), 126.9 (CH), 127.1 (CH), 128.0 (CH), 129.1 (CH), 131.5 (C), 131.5 (C), 131.5 (C), 132.6 (C), 133.0 (C), 133.2 (C), 140.5 (C), 141.6 (C), 151.6 (C), 155.5 (C═O); HRMS (EI) calcd for $C_{33}H_{31}NO_3S$ 521.20245, found 521.20278. *trans*-**14** (R_f = 0.28): ^{1}H NMR (500 MHz, $CDCl_3$) δ = 1.10−1.12 (d, J = 6.84 Hz, 3H), 1.45 (s, 9H), 1.92−1.98 (dq, J = 6.84, 6.35 Hz, 1H), 2.30−2.34 (d, J = 15.62 Hz, 1H), 3.01−3.05 (dd, J = 6.35, 15.62 Hz, 1H), 3.85 (s, 3H), 6.69−6.72 (td, J = 1.47, 7.81 Hz, 1H), 6.79−6.84 (m, 2H), 7.12−7.16 (m, 3H), 7.20−7.23 (t, J = 7.81 Hz, 1H), 7.27−7.31 (ddd, J = 1.46, 6.83, 9.76 Hz, 1H), 7.52−7.59 (m, 3H), 7.69−7.71 (dd, J = 1.46, 7.81 Hz, 1H), 9.16−9.17 (d, J = 8.30 Hz, 1H); ^{13}C NMR (100 MHz, $CDCl_3$) δ = 21.0 (CH_3), 28.7 (CH_3), 36.8 (CH_2), 58.1 (C−S), 71.2 (C−S), 81.5 (C−O), 41.5 (CH), 55.7 (OCH_3), 112.0 (CH), 112.5 (CH), 123.3 (CH), 123.6 (CH), 123.7 (CH), 124.2 (CH), 124.3 (CH), 124.6 (CH), 125.2 (CH), 126.6 (CH), 127.9 (CH), 129.0 (CH), 129.1 (CH), 131.2 (C), 131.4 (C), 131.5 (C), 133.0 (C), 133.5 (C), 137.0 (C), 140.1 (C), 141.6 (C), 151.6 (C), 156.8 (C═O); m/z (EI, %) = 521 (M^+, 57.7), 465 (100), 420 (M^+ − Boc + H, 86.8), 57 (^{t}Bu$^+$, 94.6); HRMS (EI) calcd for $C_{33}H_{31}NO_3S$ 521.20245, found 521.20287.

8. (9*Z*)- and (9*E*)-*tert*-Butyl 2-methoxy-9-(2-methyl-2,3-dihydro-1*H*-cyclopenta[*a*]naphthalen-1-ylidene)acridine-10(9*H*)-carboxylate (*cis*-10 and *trans*-10). These compounds were originally prepared as a mixture according to the procedure described for **1** starting from the mixture of *cis*-**14** and *trans*-**14** (300 mg, 0.58 mmol) and tris(4-methoxyphenyl)phosphine (243 mg, 0.69 mmol). Repeated flash chromatography (SiO_2, *n*-pentane/ether = 10:1) performed in the absence of light several times followed by additional recrystallization of the each separated isomer from propane-2-ol (30 mL) allowed to reach complete separation *cis*-**10** and *trans*-**10** one from another. *cis*-**10** (R_f = 0.32, 157 mg, 0.32 mmol, 56%) was obtained as yellowish solid: mp 198−201 °C (sealed capillary); ^{1}H NMR (500 MHz, $CDCl_3$) δ = 0.88−0.89 (d, J = 6.84 Hz, 3H), 1.59 (s, 9H), 2.65−2.68 (d, J = 15.63 Hz,

1H), 2.91 (s, 3H), 3.64−3.68 (dd, J = 6.34, 15.63 Hz, 1H), 4.38−4.43 (dq, J = 6.34, 6.84 Hz, 1H), 6.07−6.08 (d, J = 2.44 Hz, 1H), 6.60−6.62 (dd, J = 2.44, 8.79 Hz, 1H), 6.91−6.94 (t, J = 7.81 Hz, 1H), 7.08−7.10 (d, J = 8.79 Hz, 1H), 7.21−7.30 (m, 4H), 7.43−7.45 (d, J = 8.30 Hz, 1H), 7.49−7.51 (d, J = 8.79 Hz, 1H), 7.72 (d, J = 7.81 Hz, 1H), 7.73−7.74 (d, J = 8.30 Hz, 1H), 7.79−7.81 (d, J = 7.81 Hz, 1H), 7.84−7.86 (d, J = 7.81 Hz, 1H); ^{13}C NMR (100 MHz, $CDCl_3$) δ = 19.2 (CH_3), 28.4 (CH_3), 37.7 (CH), 40.1 (CH_2), 55.1 (OCH_3), 81.5 (C−O), 110.8 (CH), 113.9 (CH), 123.8 (CH), 124.0 (C), 124.3 (CH), 124.7 (CH), 124.9 (CH), 125.2 (CH), 125.5 (CH), 126.1 (CH), 126.2 (CH), 126.9 (CH), 127.8 (CH), 128.7 (C), 130.0 (CH), 132.4 (C), 132.9 (C), 135.4 (C), 135.5 (C), 137.8 (C), 139.6 (C), 145.2 (C), 146.1 (C), 152.7 (C), 156.5 (C═O); (2′*S*)-(*M*)-*cis*-**10**, UV/vis (*i*-pentane, 25 °C, λ ($\varepsilon \times 10^4$), nm) 255 (2.29), 321 (0.90), 367 (1.94); CD (*i*-pentane, 25 °C, λ ($\Delta\varepsilon$), nm) 227 (−103.4), 255 (+39.2), 282 (+27.3), 313 (+10.6), 363 (−2.8); HRMS (EI) calcd for $C_{33}H_{31}NO_3$ 489.23037, found 489.22896. Anal. Calcd for $C_{33}H_{31}NO_3$: C, 80.78; H, 6.53; N, 2.83. Found: C, 80.72; H, 6.49; N, 2.79. *trans*-**10** (R_f = 0.30, 78 mg, 0.16 mmol, 28%) was obtained as white solid: mp 199−202 °C (sealed capillary); ^{1}H NMR (500 MHz, $CDCl_3$) δ = 0.90−0.91 (d, J = 6.83 Hz, 3H), 1.60 (s, 9H), 2.64−2.67 (d, J = 15.63 Hz, 1H), 3.65−3.69 (dd, J = 6.34, 15.63 Hz, 1H), 3.87 (s, 3H), 4.37−4.43 (dq, J = 6.34, 6.83 Hz, 1H), 6.51−6.55 (t, J = 7.31 Hz, 1H), 6.60−6.62 (d, J = 7.81 Hz, 1H), 6.83−6.85 (dd, J = 2.93, 8.79 Hz, 1H), 6.86−6.89 (t, J = 8.30 Hz, 1H), 7.02−7.06 (t, J = 8.30 Hz, 1H), 7.06−7.08 (d, J = 8.79 Hz, 1H), 7.18−7.21 (t, J = 8.30 Hz, 1H), 7.42 (d, J = 2.44 Hz, 1H), 7.43−7.45 (d, J = 8.30 Hz, 1H), 7.59−7.61 (d, J = 8.30 Hz, 1H), 7.71−7.75 (m, 3H); ^{13}C NMR (100 MHz, $CDCl_3$) δ = 19.1 (CH_3), 28.4 (CH_3), 38.1 (CH), 40.3 (CH_2), 55.7 (OCH_3), 81.5 (C−O), 111.1 (CH), 111.2 (CH), 128.8 (CH), 124.0 (C), 124.2 (CH), 124.5 (CH), 124.7 (CH), 125.3 (CH), 125.9 (CH), 126.0 (CH), 126.5 (CH), 127.1 (CH), 127.9 (CH), 128.6 (C), 130.1 (CH), 132.7 (C), 135.6 (C), 136.9 (C), 137.2 (C), 139.2 (C), 145.2 (C), 146.2 (C), 152.6 (C), 156.8 (C═O); m/z (EI, %) = 489 (M^+, 34.9), 433 (100), 388 (M^+ − Boc + H, 85.6), 141 (33.7), 57 (^{t}Bu$^+$, 63.8); (2′*S*)-(*M*)-*trans*-**10**, UV/vis (*i*-pentane, −143 °C, λ ($\varepsilon \times 10^4$), nm) 255 (2.72), 321 (0.95), 367 (2.03); CD (*i*-pentane, −143 °C, λ ($\Delta\varepsilon$), nm) 226 (−91.0), 258 (+58.5), 277 (+40.4), 363 (−6.5); HRMS (EI) calcd for $C_{33}H_{31}NO_3$ 489.23037, found 489.22883. Anal. Calcd for $C_{33}H_{31}NO_3$: C, 80.78; H, 6.53; N, 2.83. Found: C, 80.69; H, 6.50; N, 2.79.

Acknowledgment. The authors thank Pieter van der Meulen and Klaas Dijkstra (NMR department, University of Groningen) for assistance with NMR spectroscopy, Dr. W. R. Browne and Dr. S. R. Harutyunyan for discussion, and NanoNed and European Research Council (ERS grant 227897) for financial support.

Supporting Information Available: General experimental methods, synthetic procedures and characterization data, all spectroscopic and kinetic data of the photochemical and thermal interconversion of all new motors, as well as X-ray crystallography information of *cis*-**10**. This material is available free of charge via the Internet at http://pubs.acs.org.